How are teeth better than bone? An investigation of dental tissue diagenesis and state of preservation at a histological scale (with photo catalogue)

Hege I. Hollund, Miranda M.E. Jans and Henk Kars

1. Introduction

Ancient teeth are windows into the lives of deceased humans and animals and thus a crucial source material for archaeologists, palaeontologists, biologists and forensic scientists. In archaeological investigations, teeth are often the preferred material for analyses involving isotopic and genetic assays. For isotopic work, teeth, in comparison with bone, can yield signals from different periods of an individual's lifetime, useful in dietary reconstruction (Bocherens *et al*. 2007), climate research (Rosvold *et al*. 2010) and investigation into movement of people and animals in the past (Britton *et al.* 2009). Additionally, several authors have suggested that teeth preserve biomolecules (e.g. DNA, collagen) better than bone (Gilbert *et al*. 2005; Adler *et al*. 2011; Meyer *et al*. 2000). The assumption is that the decay-resistant enamel cover and position within the jaw protects the dentine from attack by micro-organisms and infiltrations by extraneous materials. Bioerosion will cause loss of collagen (Hedges 2002) as well as introduction of bacterial/fungal DNA and will increase porosity, leading to further contamination (Gilbert *et al*. 2005) and accelerated decay. Infiltration by humics from the soil may cause problems both for the extraction of collagen and DNA (van Klinken and Hedges 1995), whereas inorganic compounds such as iron and copper compounds may cause problems for DNA extraction (Alaeddini *et al*. 2010; Breen and Murphy 1995; King *et al*. 2009). However, few systematic comparative studies have been carried out (see review in Hollund *et al*. 2012a) and several authors have detected chemical diagenesis in tooth enamel, a dental tissue that is considered to be highly resistant to diagenesis (Sponheimer and Lee-Thorp 2006; Hinz and Kohn 2010), protecting the tooth as a whole from exogenous diagenetic agents. Furthermore, investigations into diagenetic alterations in teeth at the histological scale are scant. This is despite the importance of teeth in archaeological research and the increasing awareness of preservation issues affecting the potential for various types of analyses. An exception is a recent study by our group, comparing histological preservation in archaeological human bone-tooth pairs (Hollund *et al*. 2012a). The results supported the argument that teeth often preserve better than bone. However, the study also showed that this is not always the case and severe alterations can also occur in teeth. Thus, for teeth, as for bone, it is important to consider and investigate post-mortem alterations before making decisions on further analyses of dental tissue biomolecules and chemistry.

The current study aims to investigate in more detail diagenetic patterns observable at histological scale, using mainly the same examples of human teeth as in Hollund *et al*. (2012a). The samples were taken from a cemetery in Eindhoven, the Netherlands, dating from 1260 to 1850 AD. In addition, seven teeth, including two animal teeth, from four other sites dating from the Mesolithic to the 16th century, were available for sampling.

The aim of comparing bone and teeth in our previous paper was to answer the general question: 'Are teeth better?'. The comparative histological study pointed both to similarities and differences between dentine/cementum and bone and that this depended on taphonomic factors, including environmental conditions and fluctuations in these. The teeth were on average better, considering histological integrity and collagen preservation (Hollund *et al*. 2012a). Consequently, the follow-up question is:

How are teeth better? Detailed discussion of this was beyond the scope of our previous study. Here we will describe diagenetic patterns observed in the teeth and include a catalogue of micrographs. There are several publications reporting histological characterisation of bone diagenesis, but most relevant as a comparison in this case is the review of bone diagenesis by Jans (2005), which includes an atlas of diagenetic features. The current article seeks to provide a comparable review and atlas of the features observed in teeth. This histological study will show patterns in severity and type of degradation in the different tissues of teeth. The assemblage consists mainly of adult human teeth, with only two children's teeth and two cattle teeth. As such it does not permit consideration of differences caused by species and biological age. However, several of the teeth contained common pathologies such as caries and attrition, which allows observations of any relationships between diagenesis and pathology.

Numerous studies of bone diagenesis at histological scale (Hackett 1981; Garland 1987; Grupe and Dreser-Werringloer 1993; Jans *et al*. 2004; Hedges *et al*. 1995), have left basic questions unanswered, including which organisms are involved in bioerosion and how fast such attack is initiated and progresses post-mortem. Detailed characterisation of microbial attack within dental tissues may throw light upon the processes behind microbial skeletal tunnelling as the process takes place in a different substrate. The characterisation would seek to address questions such as:

- Where does the invasion of micro-organisms start and what is the overall pattern of attack?
- What different types of morphological alterations can be observed and what may these represent?
- Which tissues are being altered?
- How, if at all, does dental pathology affect diagenesis and can we distinguish the two from each other?

2. Histological Characterisation of Dental Diagenesis - a short review

Post-mortem microbial invasion in archaeological teeth was first described in 1864 by Carl Wedl, observing what was subsequently termed *Wedl type tunnels* (Hackett 1981), attributed in one study to fungal activity (Marchiafava *et al*. 1974). A century after Wedl, Sognnaes (1950) reported different kinds of tunnels in archaeological teeth found to penetrate both from the pulpal dentinal surface and the external cementum surface. These types of canals are similar to those observed in bone, described by Hackett (1981) as linear longitudinal and budded tunnels and thought to be the result of bacterial activity (Jackes *et al*. 2001). Microbial borings, fungal and bacterial, are also often described as *microscopical focal destruction*, or MFD (Hackett 1981). Poole and Tratman (1978) also noted focal destructions in the dentine and attributed this to actinobacteria; mycelium-producing gram-positive bacteria that are common in decaying organic material within both terrestrial and aquatic environments. Although a few more recent authors have noted destructive foci within archaeological teeth (Bell *et al*. 1991; Hillson 1986; Kierdorf *et al*. 2009), Turner-Walker (2008) is one of the few to discuss dental histological post-mortem alterations in more detail. He showed that elongated destructive foci dominate in the dentine while the destructive foci found in the cementum are of a larger globular/ampulla-shaped type. As in bone, bacterial penetration is influenced by the micro-architecture of the tissues. The differing orientation of the tunnels to the plane of the section in both bone and teeth, indicates that the bacteria follow the orientation of the collagen fibres and are able to exploit planes of weakness in the tissues (Turner-Walker 2008). After decades of research into microbial alterations in skeletal tissues, it has not yet been possible to link specific organisms to the observed tunnelling. We suspect that in future years, next-generation sequencing will begin to reveal more of the nature of the micro-organisms that colonise ancient teeth and bone. An interesting recent contribution in that respect is the study by Pitre *et al*. (2013), who characterised biofilms in ancient bones using a combination of SEM-imaging, microbe isolation techniques and DNA sequencing. Likewise, degradation experiments such as that of Turner-Walker (2012) and Fernández-Jalvo *et al*. (2010), aid in understanding features caused by early stage diagenetic processes, including alterations caused by microbes.

In addition to microbial alteration, other diagenetic features often described in bone thin-sections are expected to occur in dentine. This include generalised destruction (the loss of recognisable microstructure due to mineral dissolution) (Garland 1993), infiltrations, inclusions and micro-cracking (Jans 2005).

3. Materials and Methods

Figure 1: Map showing the location of sites sampled

Teeth were sampled from 26 human skeletons from the Eindhoven cemetery, representing different time periods and preservation states. To minimise damage to the remains, loose teeth were sampled where available. Information on whether or not teeth were *in situ* within the jaw, or loose, is noted in Table 1, along with a summary of the sample descriptions. The site and the skeletal material are described in Hollund *et al*. (2012a). A cattle tooth was sampled from the Mesolithic causewayed enclosure site at Champ Durand in southern France. Here, large cattle bone assemblages were found in the ditches surrounding the enclosure (Feulner *et al*. 2012). Another set of teeth, three human and one cattle, was available from the Roman period cemetery in Castricum, the Netherlands. A description of this site can be found in Hollund *et al*. (2012b). Human teeth were also sampled from two environmentally very different sites; a recently excavated 16th-century cemetery in the city of Zwolle, the Netherlands and a Bronze Age burial on Sai island in the Nile river, Sudan (Nubia). The site locations are shown in Figure 1.

Table 1: Sample descriptions (see also Table 2)

Sample no.	Archaeological code	Site, country	Period	Taxon	Anatomy	In situ in jaw?	Notes
EIN-01	3993	Eindhoven, NL	1500-1650 AD	Human	3rd molar, lower right	Yes	Cross-cut by other burial
EIN-02	4125	Eindhoven, NL	1500-1650 AD	Human	2nd molar, lower right	Yes	Excellent macroscopic preservation
EIN-03	4214	Eindhoven, NL	1200-1350 AD	Human	Incisor	No	Cross-cut by other burial
EIN-04	4359	Eindhoven, NL	1200-1350 AD	Human	Premolar?	No	Cross-cut by other burial

EIN-05	1390	Eindhoven, NL	1650-1850 AD	Human	Molar	No	Child
EIN-06	2179	Eindhoven, NL	1650-1850 AD	Human	M3, upper.	Yes	
EIN-07	4132	Eindhoven, NL	1500-1650 AD	Human	M1, lower left	Yes	Excellent macroscopic preservation
EIN-08	4217	Eindhoven, NL	1350-1500 AD	Human	Canine, upper right	Yes	
EIN-09	4055	Eindhoven, NL	1350-1500 AD	Human	M2, lower right	No	Cross-cut by church wall
EIN-10	3521	Eindhoven, NL	1200-1350 AD	Human	M3, upper, right	Yes	
EIN-11	4291	Eindhoven, NL	1200-1350 AD	Human	Molar	No	Poor macroscopic preservation
EIN-12	3426	Eindhoven, NL	1650-1850 AD	Human	Canine, lower left	Yes	
EIN-13	3857	Eindhoven, NL	1200-1350 AD	Human	M3, lower, right	No	Poor macroscopic preservation
EIN-14	3793	Eindhoven, NL	1350-1500 AD	Human	?Canine, lower left	Yes	Poor macroscopic preservation
EIN-15	4062	Eindhoven, NL	1500-1650 AD	Human	2nd premolar, upper left	Yes	
EIN-16	3864	Eindhoven, NL	1500-1650 AD	Human	M2, lower left	Yes	
EIN-17B	3648	Eindhoven, NL	1350-1500 AD	Human	Molar	No	Poorly preserved, some parts only silhouette
EIN-17C	3648	Eindhoven, NL	1350-1500 AD	Human	Molar	No	Poorly preserved, some parts only silhouette
EIN-18	1723	Eindhoven, NL	1350-1500 AD	Human	M3	Yes	

EIN-19	2108	Eindhoven, NL	1650-1850 AD	Human	Central incisor, right, upper	No	Excellent macroscopic preservation
EIN-20	2165	Eindhoven, NL	1650-1850 AD	Human	Molar	Yes	
EIN-21	4298	Eindhoven, NL	1200-1350 AD	Human	M1, lower right	No	Child, 7 yr old
EIN-22	3242	Eindhoven, NL	1350-1500 AD	Human	M2, lower left	No information	Excellent macroscopic preservation
EIN-23	3530	Eindhoven, NL	1650-1850 AD	Human	M2, lower left	No information	
EIN-24	3821	Eindhoven, NL	1500-1650 AD	Human	M2, lower right	No information	Coffin wood preserved
EIN-49	4360	Eindhoven, NL	1200-1350 AD	Human	nd	No	Child, no root development
CAS-01	S4 9-2-54 Sp157	Castricum, NL	Roman period	Human	4.4 (lower right)	No information	Double shallow pit burial in cemetery. Cross-cut by medieval ditch, only legs in situ
CAS-11	S114 4-1-1 Sp8	Castricum, NL	Roman period	Cattle	nd	No	Possibly dumped carcass, deliberately buried
CAS-07	S148 3-1-117 Sp80	Castricum, NL	Roman period	Human	Tooth 4.7 (lower right)	No information	Individual shallow pit burial. No visible disturbance
CAS-08	S138 3-3-331 Sp63	Castricum, NL	Roman period	Human	nd	No information	Inhumation. In refuse pit
CDU-15	CDU 78 FIII A2 - 130 CP 3.5.1.32	Champ Durand, FR	Mesolithic	Cattle	nd	No	
SAI-04	Sp 409	Sai Island, the Nile, Sudan	Bronze Age	Human	nd	Yes	

ZWO-01	Vnr 13	12 Apostelen Zwolle, NL	14th-15th cent. AD	Human Tooth 3.6	Yes

The teeth were prepared as thin-sections for light microscopy. Three samples were also prepared as polished blocks for scanning electron microscopy (SEM), which allowed chemical analyses by energy dispersive X-ray spectroscopy (EDX). Sample preparation protocols and analytical equipment is described in Hollund *et al*. (2012b) and Hollund (2013), but in short involved impregnation with a two-component epoxy and using a grinding machine equipped with a diamond grinding wheel to produce thin-sections. The SEM-EDX equipment used was a JEOL JSM-59101V fitted with an EDS detector from Thermo Scientific and Noran System Seven software.

4. Results: Observations and Photo catalogue

The following sections describe the observations made concerning both biological and non-biological diagenetic features, illustrated by micrographs. The histological indexes are reported in Table 2. In addition, results from SEM-analyses in the form of backscatter electron images (SEM-BSE) and elemental spectra (SEM-EDX) are presented.

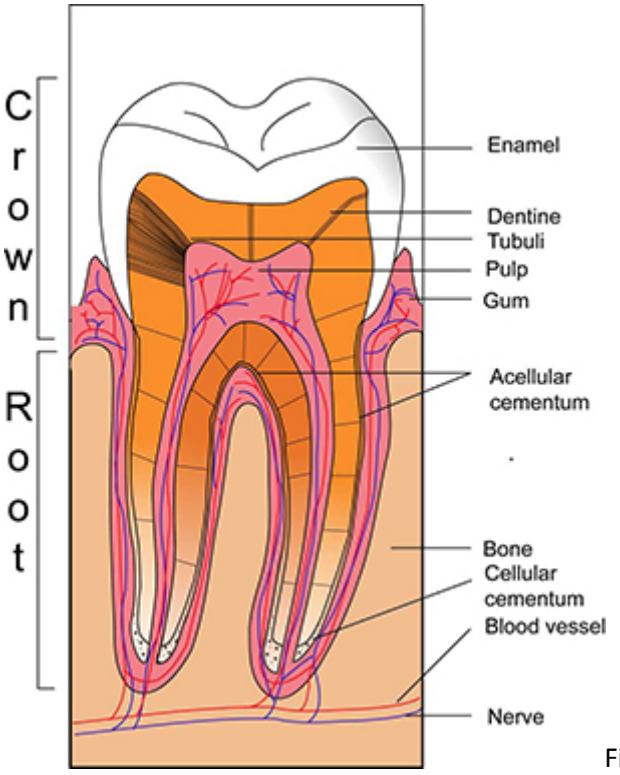

Figure 2: Schematic drawing of the longitudinal cross-section of a tooth

4.1 Dental microanatomy

Before assessing diagnetic alterations, it is necessary to be familiar with the main micro-anatomical features of teeth as seen in histological thin-sections. Teeth consist of three different types of tissues: enamel, dentine and cementum, as seen in the schematic drawing in Figure 2. The bulk of the element is made up of dentine. The roots are covered with cementum and the crown is capped by enamel. Dentine is avascular and acellular but the tissue is perforated by long odontoblast processes connected to cells within the pulp cavity. These tubuli are similar in diameter to bone canaliculi and connect the dentine to the vascular system. The cementum is partially cellular, containing cementum-forming cells

called cementocytes. The enamel is almost entirely inorganic and is a denser and more crystalline material than the other tissues (Hillson 1986). Figures 3 to 7 show micrographs that illustrate micro-anatomical features of teeth as seen in longitudinal cross-sections of whole teeth.

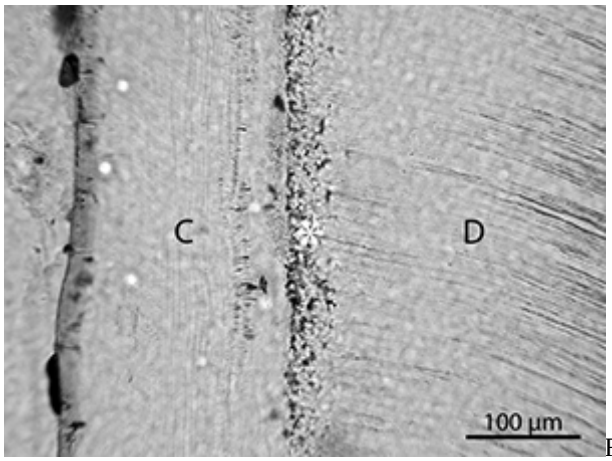

Figure 3: Acellular cementum and dentine. The asterisk marks what is called the *granular layer of Tomes*. Several interpretations exist for these structures. Recently it has been described as an enamel-like, hypermineralised zone containing little organics (Cherian 2011). Note the thinning of the dentinal tubuli close to the cementum and their fine lateral branches

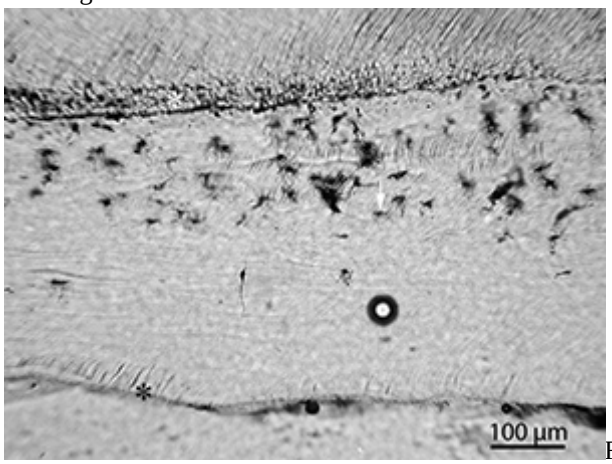

Figure 4: Cellular cementum with cementocyte lacunae (arrow). These are the lacunae of the former cementocytes, collagen-producing cells that become entrapped in the extracellular matrix they excrete during cementogenesis. The canaliculi of cementocytes communicate but are not part of an inter-connected network that extends all the way to the surface, as is the case for bone. Nourishment is believed to occur by diffusion and the deeper cementocytes may not be vital. Most of the canaliculi point toward the tooth surface (Nanci 2003). The black asterisk marks the cementum surface and the white the *granular layer of Tomes* at the cemento-dentinal junction

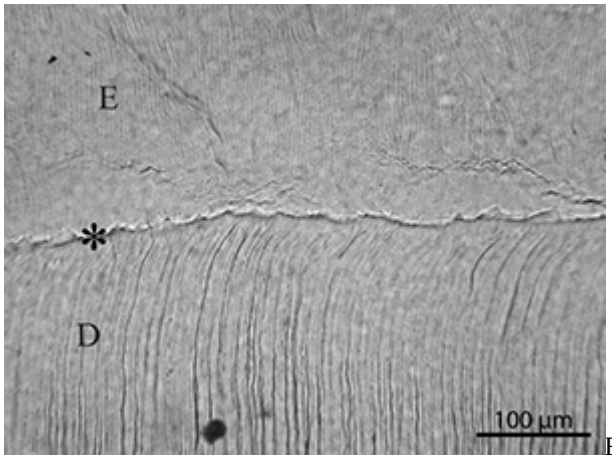

Figure 5: The dentino-enamel junction appear as a well-defined scalloped border (asterisk)

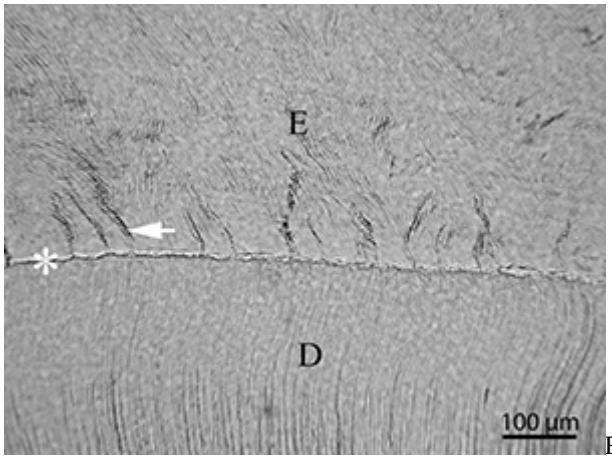

Figure 6: Tufts (arrow) crossing the dentino-enamel junction (asterisk). Tufts appear as hair-thin brushes that branch out from the junction and into the enamel. The tufts contain greater concentrations of enamel proteins than the rest of the enamel (Nanci 2003)

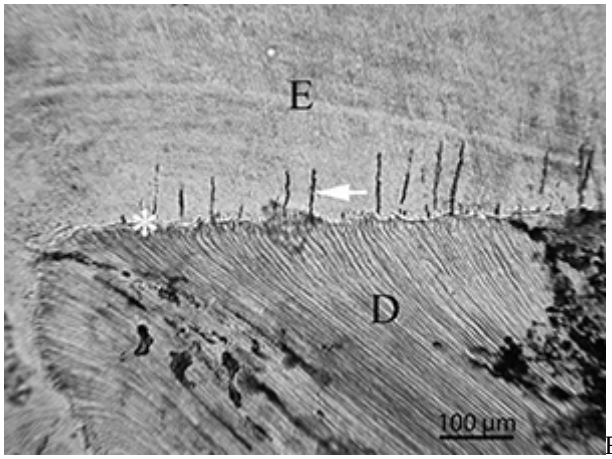

Figure 7: Spindles (arrow) crossing the dentino-enamel junction (asterisk) are remains of odontoblast processes that become trapped when enamel formation begins (Nanci 2003)

4.2 Bioerosion

In the transversal thin sections of the Eindhoven bone samples, microbial tunnelling was observed as Hackett's budded and linear longitudinal tunnels. The tunnels in the dentine and cementum appear largely similar, with a similar morphology and size to those in bone. Several of the teeth displayed possible analogues to the Wedl type 2 tunnels found in bone (Trueman and Martill 2002) in the form of enlarged canaliculi within the cementum. Within the dentine, destruction also appeared in the form of enlarged dentinal tubuli.

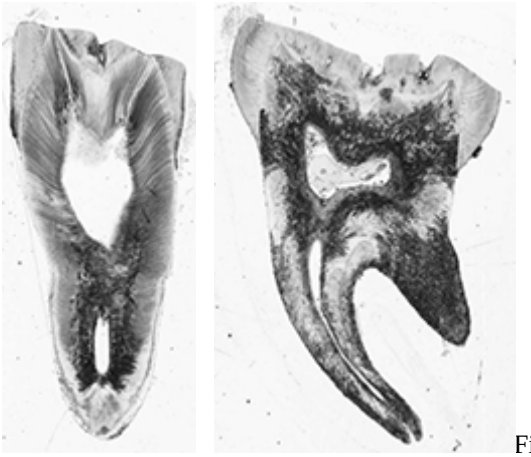

Figure 8: Scanned thin-section of sample EIN-15 showing the pattern of microbial tunnelling. The tunnels (dark areas) are mainly found within the cementum, the apex (root tip) and along the root canal Figure 9: Scanned thin-section of sample EIN-22. Here, the attack is more extensive than in EIN-15 (Figure 8) and the microbes are also entering from the surface of the pulp cavity penetrating the whole way to the dentino-enamel junction

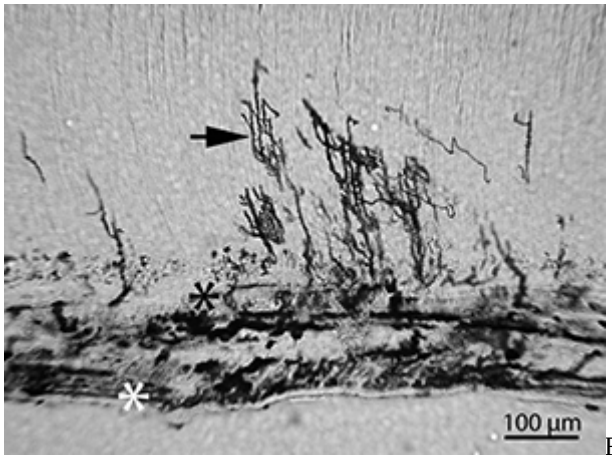

Figure 10: Micrograph of sample EIN-23. The cementum is completely bioeroded, mainly in the form of globular MFD. Despite the cemento-dentinal junction (black asterisk), the bacteria are penetrating into the dentine. The micro-organisms seem to enter the tooth at the cementum surface (white asterisk). Tunnelling into the dentine is in the form of enlarged dentinal tubuli (arrow) with branches. See also detail in Figure 16

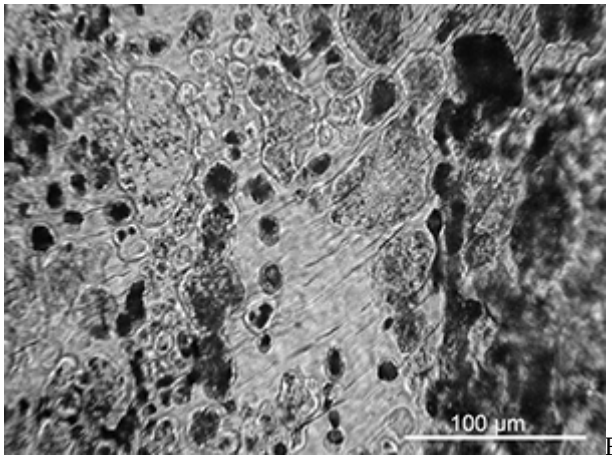

Figure 11: Micrograph of sample EIN-05 showing globular-shaped tunnels within the dentine. These are of the same size and shape as the linear longitudinal tunnels (approximately 10 µm) and budded tunnels (up to 100s of µm) seen in bone. In the middle of the image a pristine area of dentine can be seen, with the dentinal tubuli clearly visible

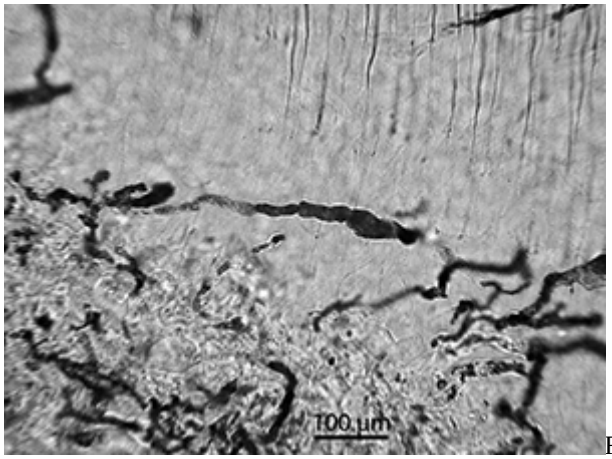

Figure 12: Micrograph of sample EIN-16. Destructive foci are observed as several connected oblong shapes

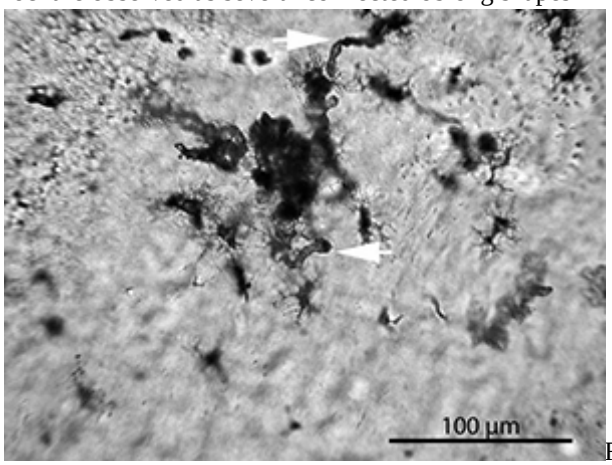

Figure 13: Micrograph of sample EIN-23. Elongated destructive foci (arrows) stretch out from cementocyte lacunae and cancaliculi

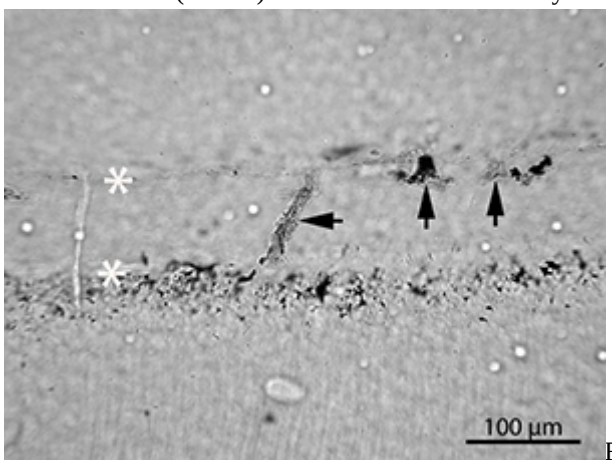

Figure 14: Micrograph of sample EIN-23. Three destructive foci within the cementum where the micro-organisms seem to have entered from the cementum surface. The white asterisks mark the cementum surface and the cemento-dentinal junction

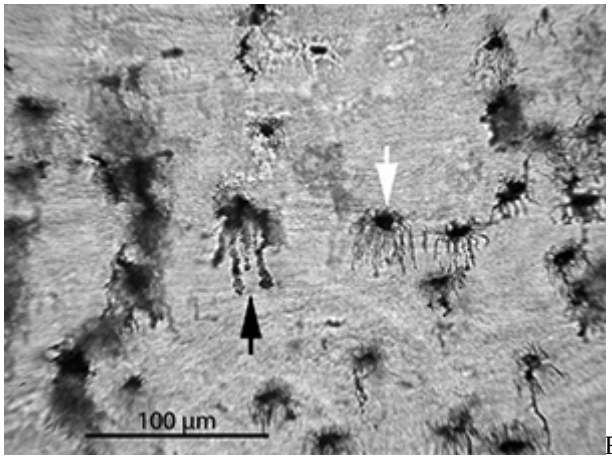

Figure 15: Micrograph of sample EIN-04. What can be described as Wedl type 2 tunnels are found within the cementum. These appear as enlarged canaliculi, first described in bone by Trueman and Martill (2002). However, these may also be caused by acid etching, as suggested by Fernández-Jalvo *et al*. (2010) for bone samples. This may also be the case here (black arrow). Alternatively, the canaliculi may appear enlarged whereas this is caused by staining along the canaliculi. The fine central line may be the original canaliculi and the broader darker band being caused by infiltrations. The white arrow indicates an unaffected cementocyte lacuna

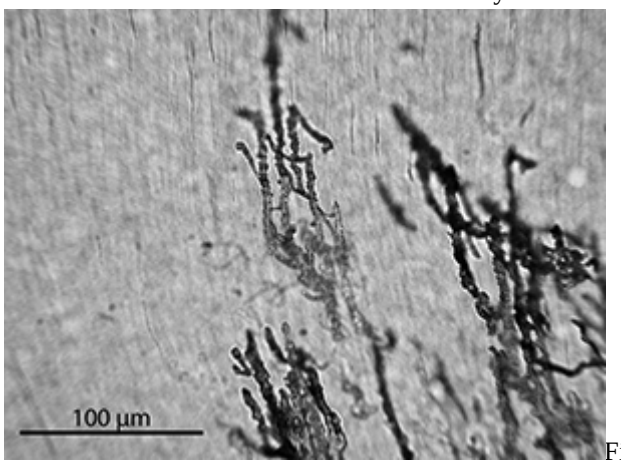

Figure 16: Micrograph of sample EIN-23. Destructive foci in the dentine appear as enlarged dentinal tubuli and lateral branches

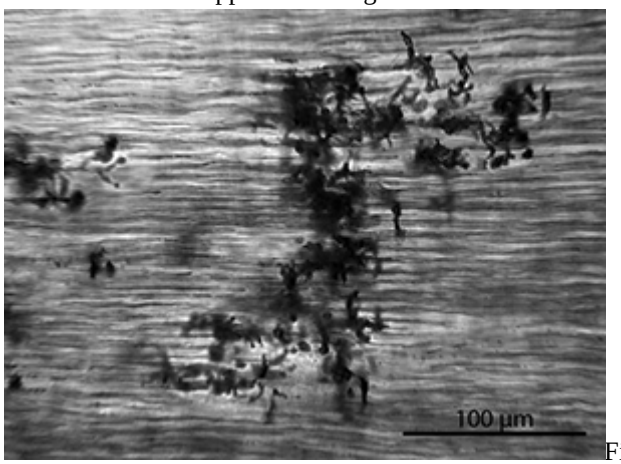

Figure 17: Micrograph of sample EIN-23. Destructive foci in the form of enlarged lateral branches of the dentinal tubuli

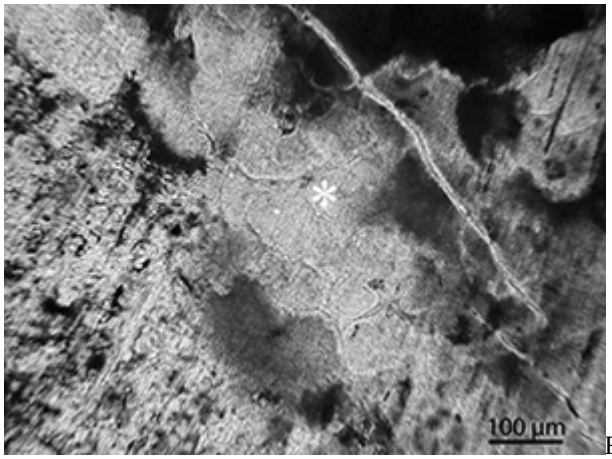

Figure 18: Micrograph of sample EIN-22. An area with large, globular MFD with a grainy interior can be seen in the middle of the image (asterisk). The pattern of the dentine microstructure is visible within the foci, in a way similar to lamellar tunnels in bone (Hackett 1981) and what was observed by Bell *et al*. (1991) in dentine. See also SEM-BSE images in Figures 19 and 20

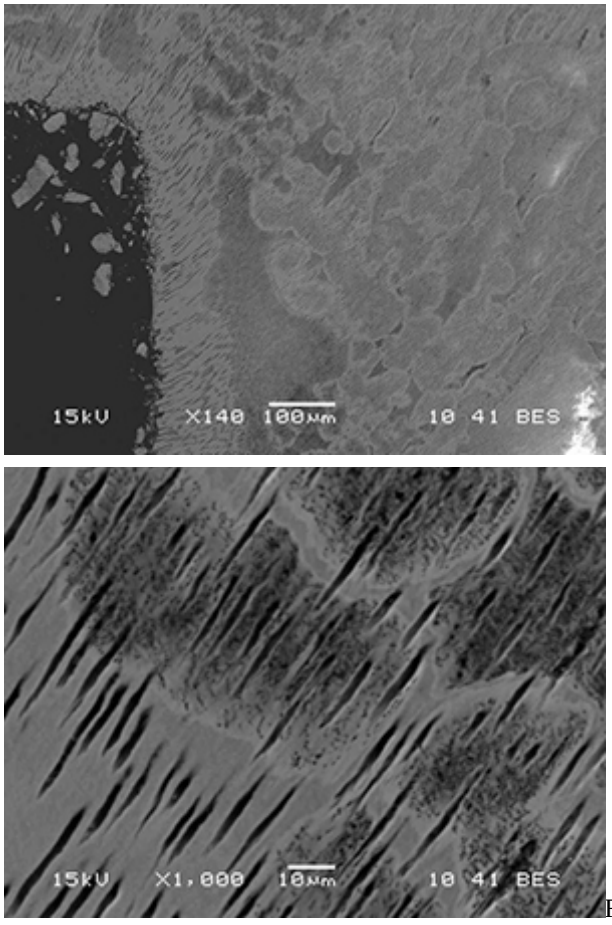

Figures 19: SEM-BSE image of the large MFD seen in Figure 18. The SEM-BSE images show that the destructions consist of a demineralised area with a border of more highly mineralised material. See SEM-BSE image in Figure 20 for higher magnification. (Image credit: H. Hollund)

Figure 20: SEM-BSE image of the large MFD seen in Figure 18 and 19. At this level of magnification it is possible to see that the interior of the MFD contains numerous fine pores (roughly 1 micron across), as found within bone MFD by Jackes et al. (2001), believed to represent bacterial tunnels. (Image credit: H. Hollund)

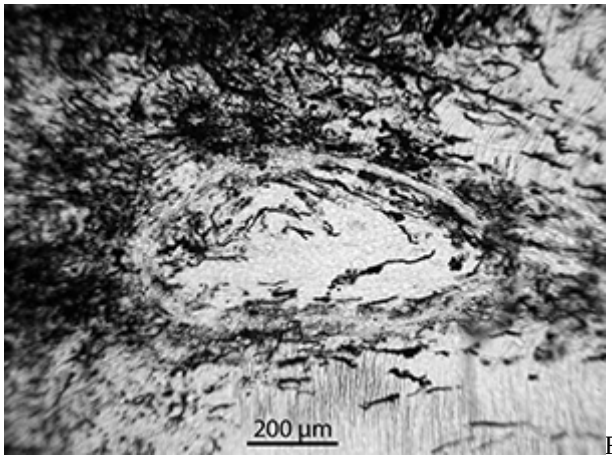

Figure 21: Micrograph of sample EIN-06. As pathologies will change the physico-chemical and/or microstructural characteristics of teeth, these may also affect the pattern of microbial attack. Here, a circular deformation is visible within the dentine; a pulp stone. These may arise as an age change or accompany inflammatory or degenerative changes in the pulp. Calcification of the pulp results in the formation of discrete, approximately circular mineralised masses which may later be incorporated into the dentine (Marsland and Browne 1975). The microbial tunnelling can be seen to follow the circular lamellar microstructure of the imbedded pulp stone

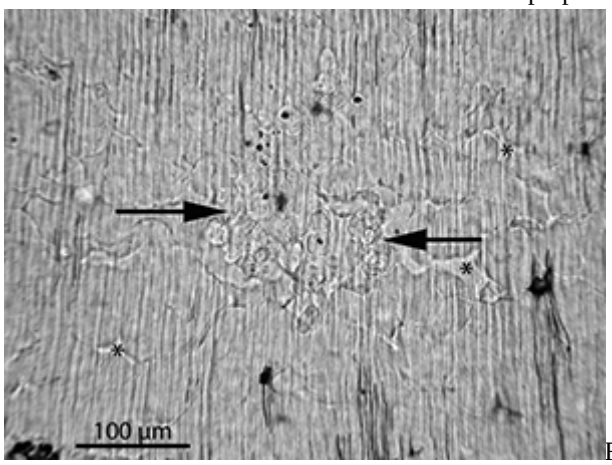

Figure 22: Micrograph of sample EIN-15. This sample displays another commonly occurring pathology, a developmental defect leading to zones of interglobular and globular dentine. These are areas of unmineralised or hypomineralised dentine where globular zones of mineralisation have failed to fuse into a homogeneous mass within mature dentine. The condition is especially prevalent in human teeth as a result of vitamin D deficiency or exposure to high levels of fluoride at the time of dentine formation (Nanci 2003). In a few samples, microbes seem to have targeted the less mineralised inter-globular dentine, as can be seen in this micrograph. The two arrows mark a cluster of MFD located in an area with inter-globular dentine. Inter-globular areas are indicated with an asterisk. These MFD are located in an area of the crown dentine, directly beneath an enamel lesion. This tooth displays otherwise dense bioerosion around the root canal and in the cementum, while there are few MFD above the pulp cavity. This may suggest that the MFD in this area were caused by micro-organisms that entered via the lesion

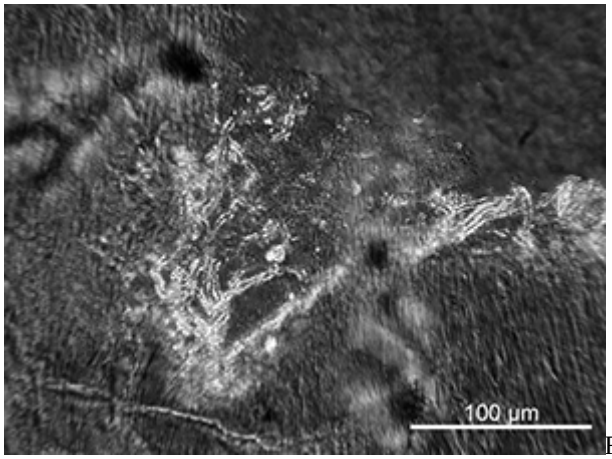

Figure 23: Micrograph of sample CDU-15, viewed in polarized light. This is a Neolithic cattle tooth, the only sample to display clearly identifiable fungal tunnelling. Round, transparent fungal structures can be seen, as well as hyphae/tunnels penetrating into the dentine from the pulp cavity surface, appearing as the characteristic Wedl type tunnels (Hackett 1981; Marchiafava *et al*. 1974; Jans 2005). The hyphae/tunnels are clearly visible in polarized light as they are lined with a birefringent material, possibly calcite as this is a known precipitate on and in soil fungal structures (Burford *et al*. 2006). See also Figures 40, 41, 42 and 43.

4.3 Inclusions and infiltrations

Several of the teeth contained orange and opaque irregularly shaped inclusions within vascular canals, osteocytes, canaliculi and dentinal tubules. These were found by chemical analysis (SEM-EDX) of selected Eindhoven samples to contain iron and manganese (see Figure 32). Birefringent material, most likely calcite, was also observed filling microbial tunnels and pores in a couple of teeth. In addition, possible calcite-containing inclusions were found within the pulp cavity. Inclusions of framboidal pyrite (FeS2) were observed in one tooth (Figures 24-26). Both bones and teeth from Eindhoven were affected by orange and brown staining to varying degrees. This may be due to infiltrations by metal compounds and/or humic factors. Chemical analysis of infiltrations observed in four teeth and three bone samples from the site detected iron and manganese (Figure 35). Most samples contained remains of various fungal structures within canals and cavities.

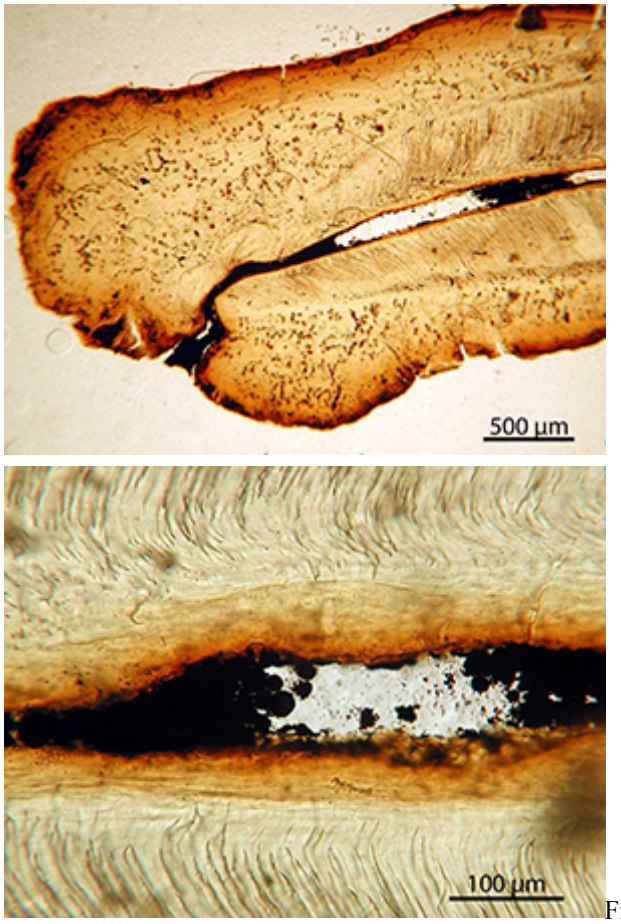

Figure 24: Micrograph of ZWO-01. This human tooth contained many framboidal pyrite (FeS2) grains on the surface of the pulp cavity and root canals, in places almost completely filling the root canals. The cementum and dentine of this tooth is stained yellow and orange indicating infiltration by iron compounds, possibly a result of partial oxidation of pyrite (see discussion in Hollund et al. 2012b). See also detail in Figure 25. (Image credit: H. Hollund)

Figure 25: Micrograph of ZWO-01. Detail of the same tooth as shown in Figure 24. This human tooth contained many framboidal pyrite (FeS2) grains on the surface of the pulp cavity and root canals, in places almost completely filling the root canals. The cementum and dentine of this tooth is stained yellow and orange indicating infiltration by iron compounds, possibly a result of partial oxidation of pyrite (see discussion in Hollund et al. 2012b). (Image credit: H. Hollund)

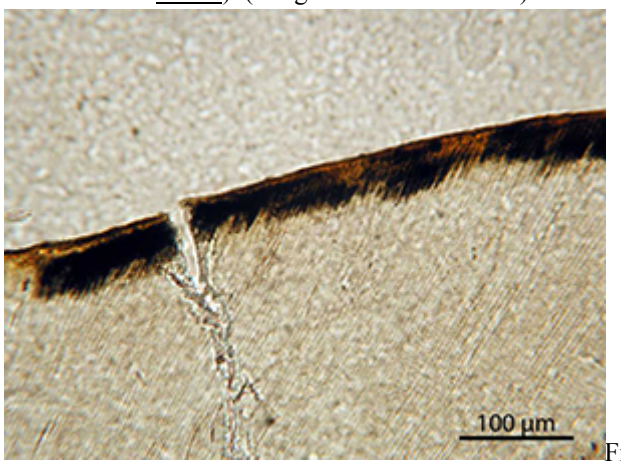

Figure 26: Micrograph showing an area of the enamel surface of ZWO-01 which is stained black and orange, possibly infiltrated by pyrite and iron oxides (see also Figures 24 and 25)

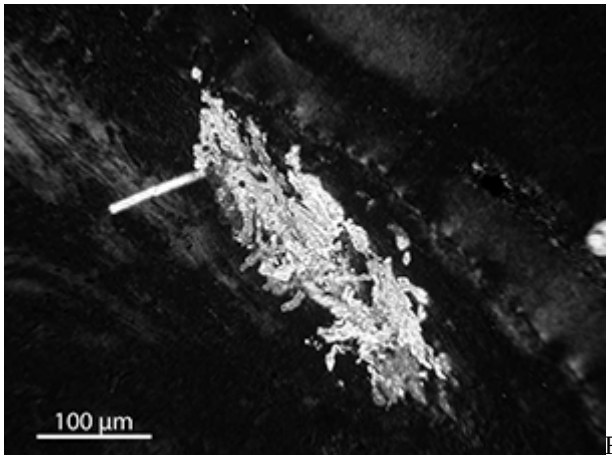

Figure 27: Micrograph of sample EIN-10 in polarized light. Empty microbial tunnels are filled with a birefringent material. Analysis by SEM-EDX detected calcium, carbon and oxygen (Figure 29); most likely calcite (see also Figure 28)

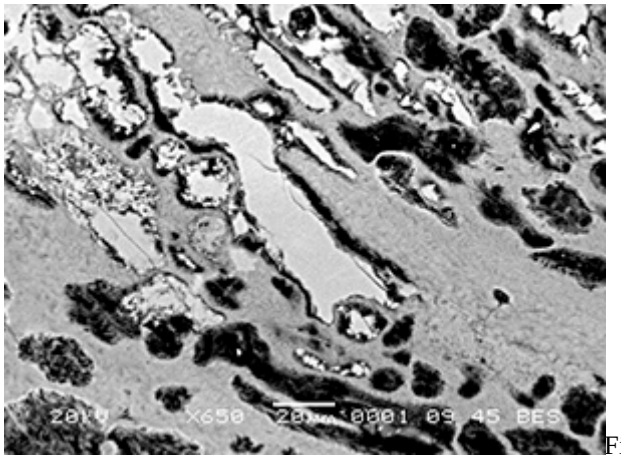
Figure 28: SEM-BSE image of sample EIN-10. Empty MFD are filled by dense material, probably calcite, as suggested by the birefringence in polarized light (see Figure 27) and SEM-EDX analysis (Figure 29)

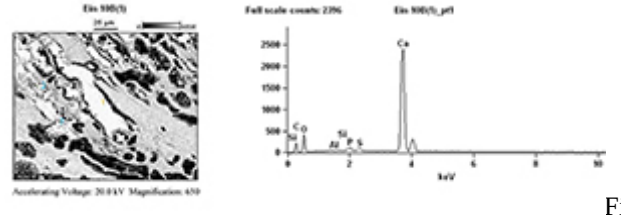
Figure 29: SEM-EDX results; chemical spot analysis of inclusions in empty MFD, sample EIN-10 (see Figures 26-28)

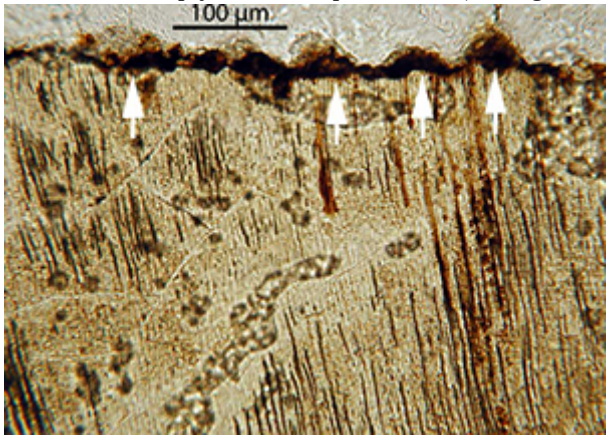

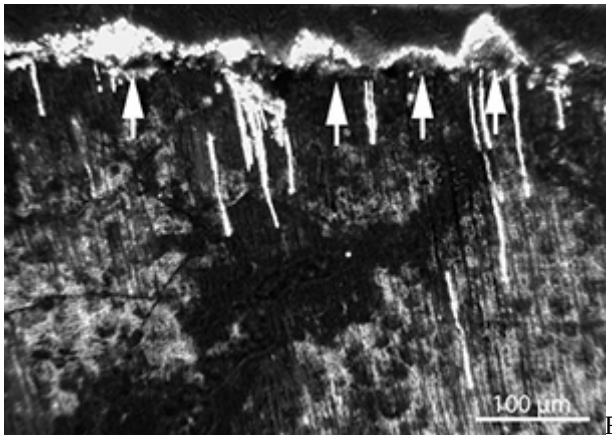

Figure 30: Micrograph of sample EIN-13 in normal light. Small (approximately 14 µm) orange and translucent pyramid-shaped nodules are found, sitting on the surface of the pulp cavity and root canal. Some of the dentinal tubuli stretching out from the cavity are also filled with orange material. This material shows birefringence in polarized light (Figure 31) and was found by SEM-EDX to contain calcium, carbon, oxygen and sometimes manganese, iron and phosphorus (Figure 32). (Image credit: H. Hollund)

Figure 31: Micrograph of sample EIN-13 in polarized light, showing that some of the inclusive material seen in Figure 30 is birefringent. This material was found by SEM-EDX to contain calcium, carbon, oxygen and sometimes manganese, iron and phosphorus (Figure 32). (Image credit: H. Hollund)

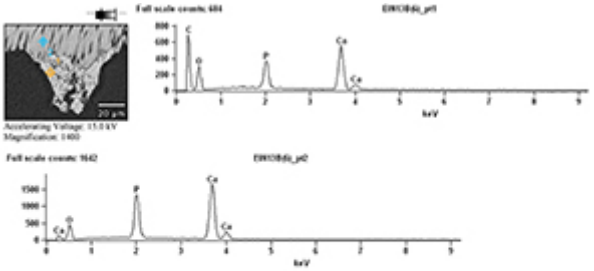

Figure 32: SEM-EDX results; chemical spot analysis of inclusions in EIN-13 (see Figures 30 and 31)

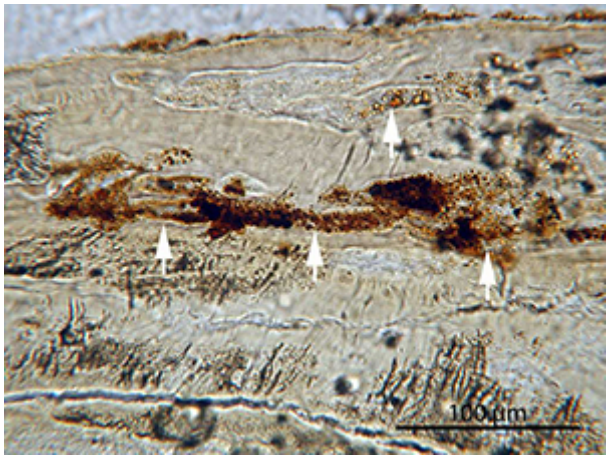

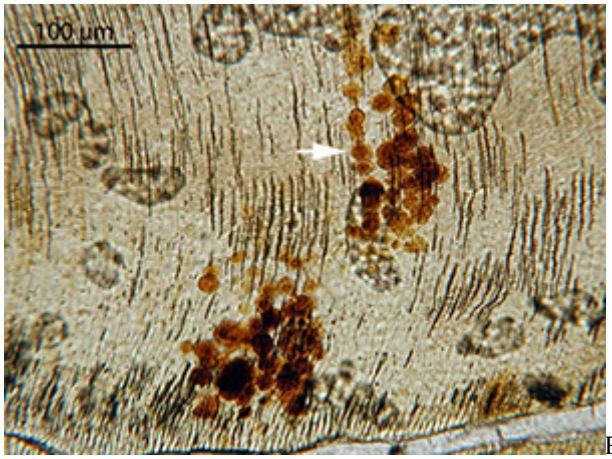

Figure 33: Micrograph of sample EIN-13. The sample contains orange perfectly round inclusions (arrows) and roughly circular stains (see Figure 34). These were found by SEM-EDX to contain iron and manganese (Figure 35). The inclusions are found within empty MFD in the cementum and dentine, whereas the stains mainly seem to follow the length of the dentinal tubuli. (Image credit: H. Hollund)

Figure 34: Micrograph of sample EIN-13. The sample contains roughly circular stains in addition to the round inclusions seen in Figure 34. Both stains and inclusions were found by SEM-EDX to contain iron and manganese (Figure 35). The inclusions are found within empty MFD in the cementum and dentine, whereas the stains mainly seem to follow the length of the dentinal tubuli. (Image credit: H. Hollund)

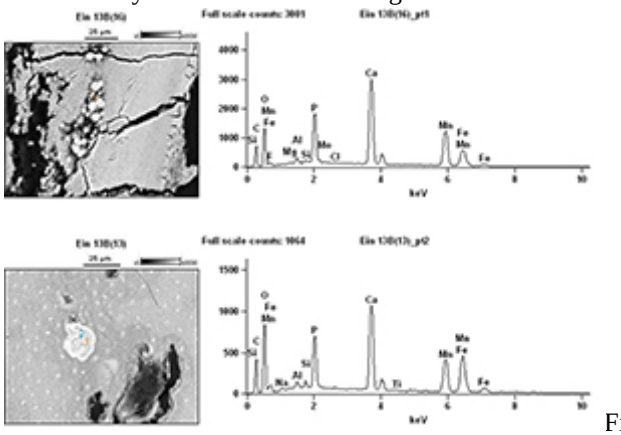
Figure 35: SEM-EDX results, inclusions and stains in EIN-13 (see also micrographs, Figures 33 and 34)

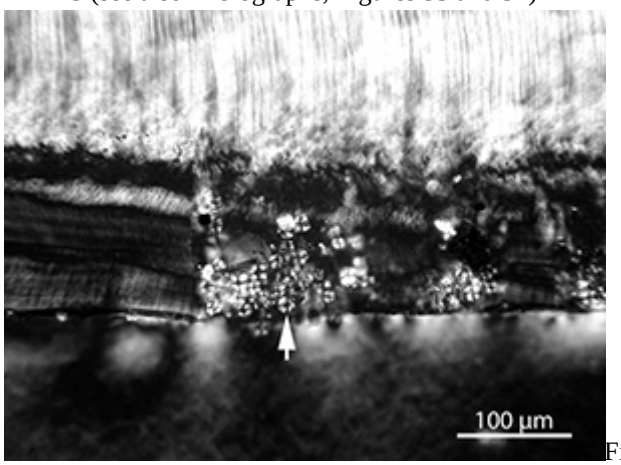

Figure 36: Micrograph of sample EIN-09 in polarized light, showing starch-grains within a crack in the cementum surface. The grains display the starch-specific extinction cross in polarized light (Piperno *et al*. 2004)

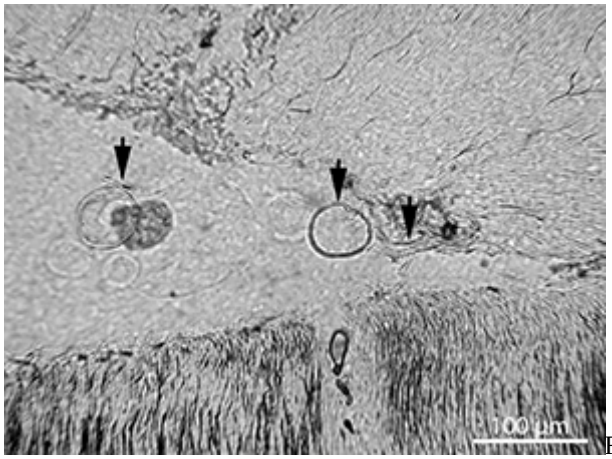

Figure 37: Micrograph of sample EIN-08, with remains of fungal fruiting bodies and fungal hyphae (arrows) within the pulp cavity

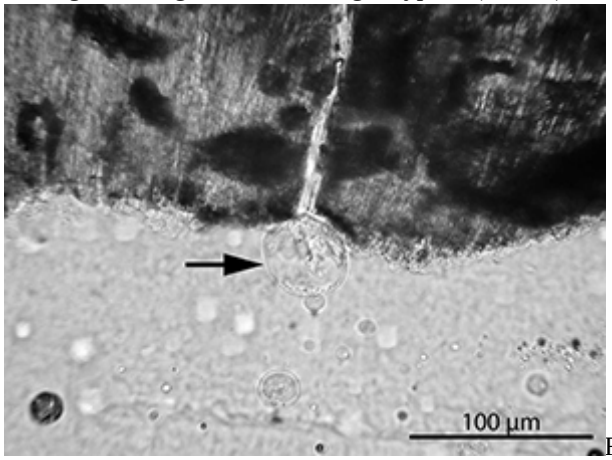

Figure 38: Fungal fruiting body on pulp cavity surface of EIN-24. The hyphae is located in a crack in the dentine

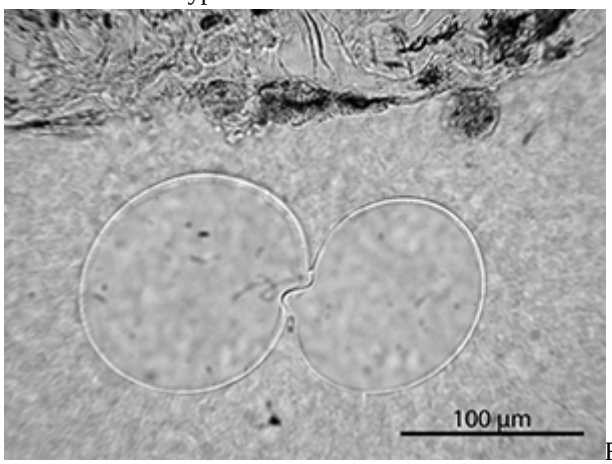

Figure 39: Yeast cells within the pulp cavity of cattle tooth CDU-15. This double form is a yeast cell reproducing by a division process called budding

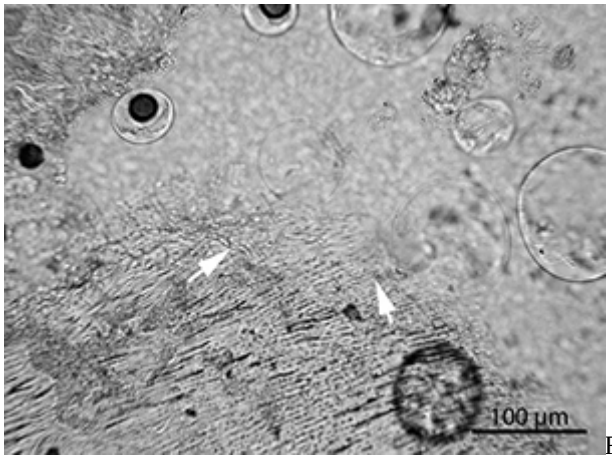

Figure 40: Micrograph of sample CDU-15 showing transparent, round fungal structures within the pulp cavity. Tunnels (white arrows) can be seen penetrating the dentine. As seen in Figure 23, the hyphae/tunnels are lined with birefringent material, probably calcite and are thus visible in polarized light (Figure 41)

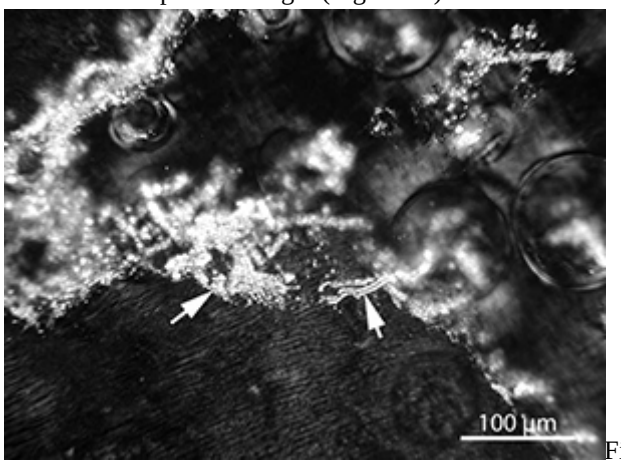

Figure 41: Micrograph of sample CDU-15, same view as Figure 40 but in polarized light. The tunnels, which seem to be caused by the action of fungal hyphae, are lined with a birefringent material that is visible in polarized light (see also detail in Figure 23).

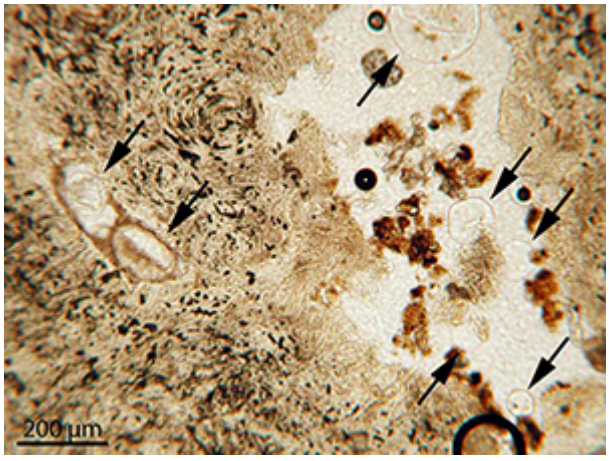

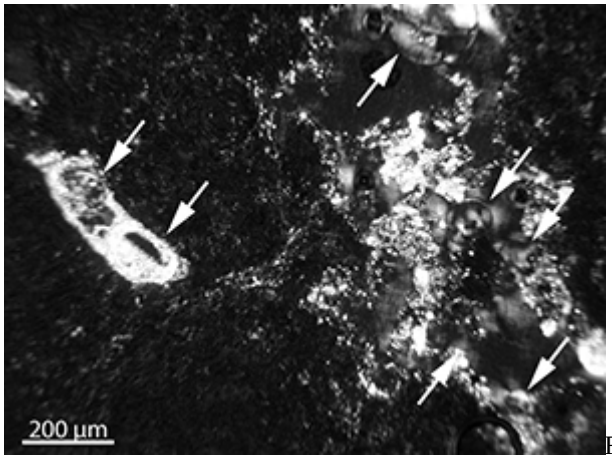

Figure 42: Micrograph of sample CDU-15, viewed in normal light. In normal light, fungal fruiting bodies (arrows) are seen within pores/cracks in the dentine, associated with masses of orange and translucent material. This material displays a bright white birefringence in polarized light. As with the fungal hyphae seen in Figure 41, one of the fungal fruiting bodies is lined with the material. No analyses were carried out but it is likely that this is calcite, with some compounds containing iron and/or manganese, as seen for sample EIN-13 (Figures 30, 31, 32) and EIN-10 (Figures 27, 28, 29). (Image credit: H. Hollund)

Figure 43: Micrograph of sample CDU-15, viewed in polarized light, showing that some of the fungal fruiting bodies (arrows) also seen in Figure 42, are lined with a bright white birefringent material. No analyses were carried out but it is likely that this is calcite, with some compounds containing iron and/or manganese, as seen for sample EIN-13 (Figures 30, 31, 32) and EIN-10 (Figures 27, 28, 29). (Image credit: H. Hollund)

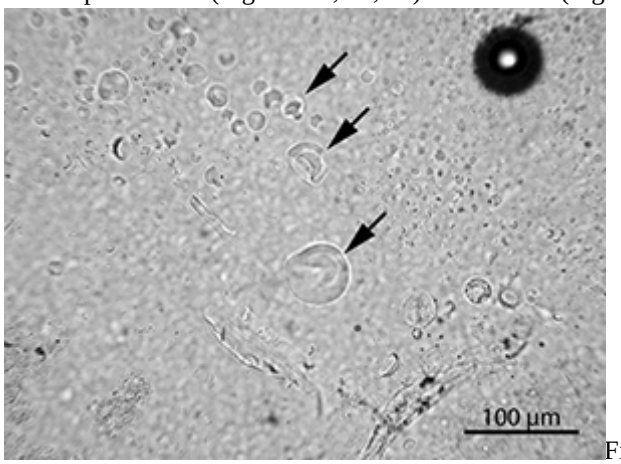

Figure 44: Micrograph of sample CDU-15 showing fungal spores within the pulp cavity.

4.4 Generalised destruction and cracking

Since dentine and cementum are chemically similar materials to bone, these are also prone to mineral dissolution and low pH. This was seen in 12 samples (35%) and is indicated by low GHI and high OHI, since this former index records both bioerosion and generalised destruction. Microcracking was not observed in dentine/cementum of any of the teeth, but large cracks are found, often in conjunction with generalised destruction.

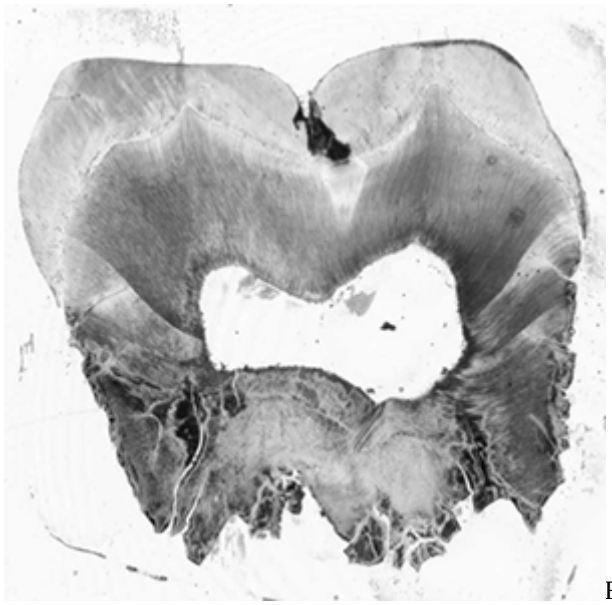

Figure 45: Scanned thin-section of EIN-17 illustrating the effects of an extreme corrosive environment that has caused generalised destruction and complete loss of a large part of the roots. Despite this, the dentine directly beneath the enamel crown remains well-preserved, testifying to the resilience of enamel and the efficient protection it provides. A caries lesion can also be seen in the enamel. This has caused some staining and reaction in the dentine

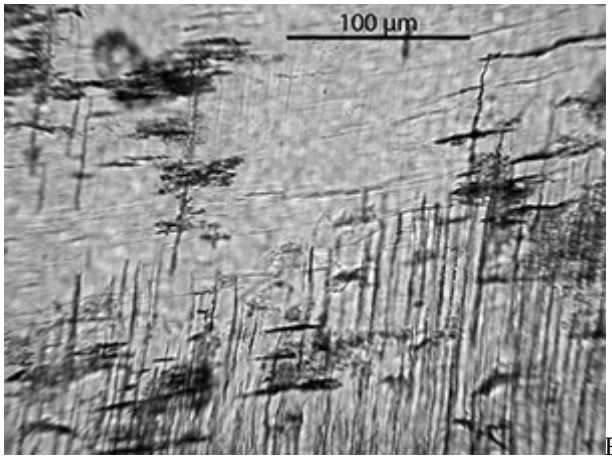

Figure 46: Micrograph of sample EIN-11 showing the effect of generalised destruction on the dentinal microstructure. The striated structure of the dentine has 'faded' in the upper half of the image. In the lower half, the tubuli and their lateral branches, appear stained and possibly enlarged. It is not possible to determine whether or not this is due to acid etching alone, or bioerosion prior to the etching

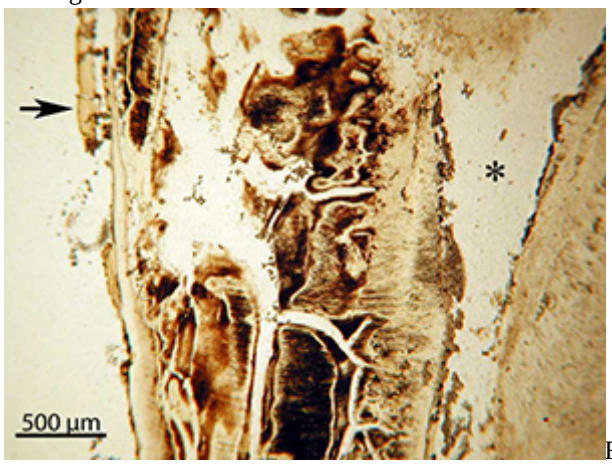

Figure 47: Micrograph of sample EIN-03. An area of generalised destruction, including staining and large cracks is shown. The cementum is lost in some areas and is detaching at the cemento-dentine junction (arrow). Sample preparation may also have caused part of this. The

asterisk marks the root canal

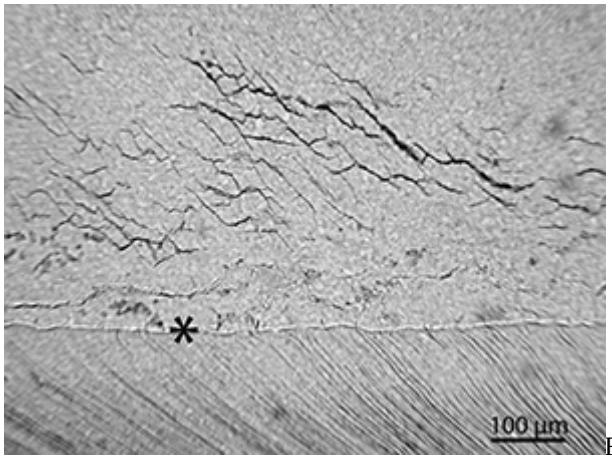

Figure 48: Micrograph of EIN-08. Micro-fissures are present in the enamel. The enamel of the teeth studied was frequently cracked to different degrees.

4.5 Diagenesis and pathologies

Several types of pathologies were observed and are illustrated here, to allow readers to identify this as non-diagenetic. It is not possible to establish, however, whether superficial etching of the enamel surface is pathology, or diagenetic in nature.

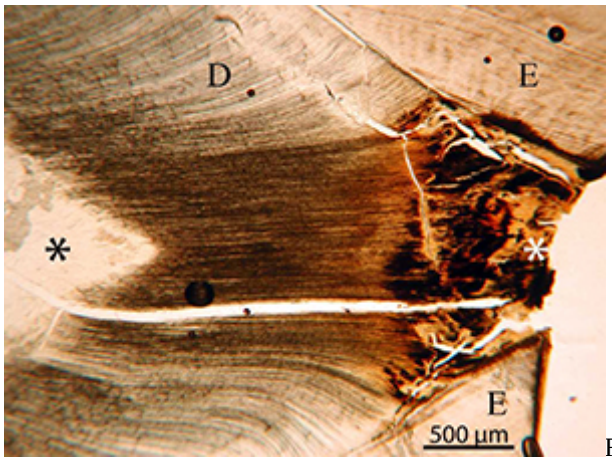

Figure 49: Micrograph of sample EIN-04. In this tooth the crown enamel has been worn down to the dentine during life and the exposed dentine is affected by orange staining and generalised destruction (white asterisk). This is at least partially pathological, seen by the tertiary, or reparative, dentine (black asterisk). This will form as reaction to stimuli such as caries or attrition and will be produced only by the cells affected by the stimulus (Nanci 2003)

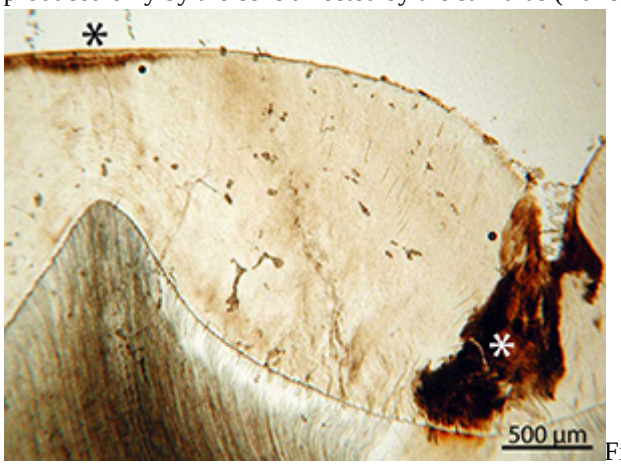

Figure 50: Micrograph of sample EIN-17. The white asterisk marks an enamel caries lesion, clearly identifiable with a reaction (orange staining) in the dentine underneath (Marsland and Browne 1975). It is not possible to determine whether or not the enamel surface

etching and staining (black asterisk) is a smooth surface lesion, or diagenetic in origin

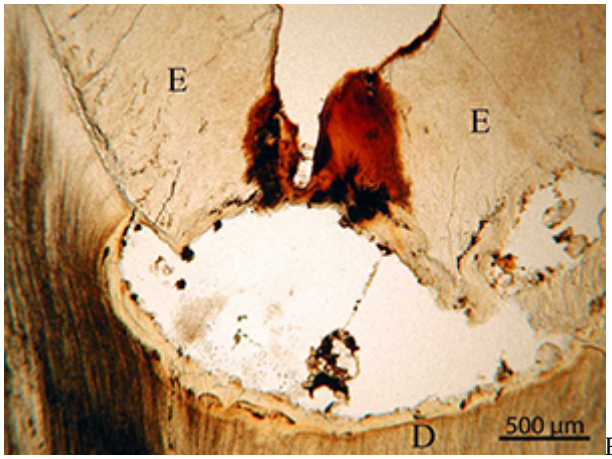

Figure 51: Micrograph of sample EIN-20. An extensive lesion of the dentine has undermined the enamel adjacent to the fissure. Such lesions may cause demineralisation of a large area directly underneath it (Marsland and Browne 1975). The lesion contains inorganic diagenetic inclusions

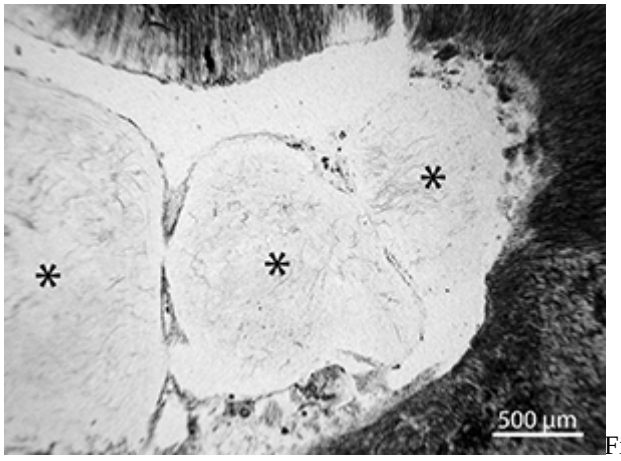

Figure 52: Micrograph of sample EIN-20. Three large pulp stones (asterisks) within the pulp cavity. These may arise as an age change or accompany inflammatory or degenerative changes in the pulp. Calcification of the pulp results in the formation of discrete, approximately circular mineralised masses (Marsland and Browne 1975). Finally, these may be completely incorporated into the dentine, as seen in Figure 21

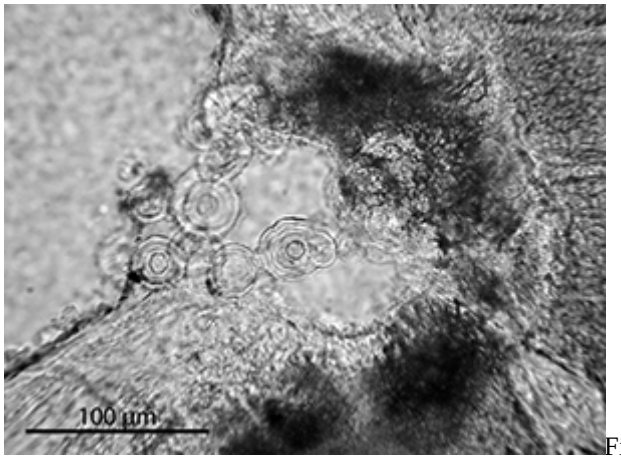

Figure 53: Micrograph of sample SAI-04. A cluster of small pulp stones within the pulp cavity

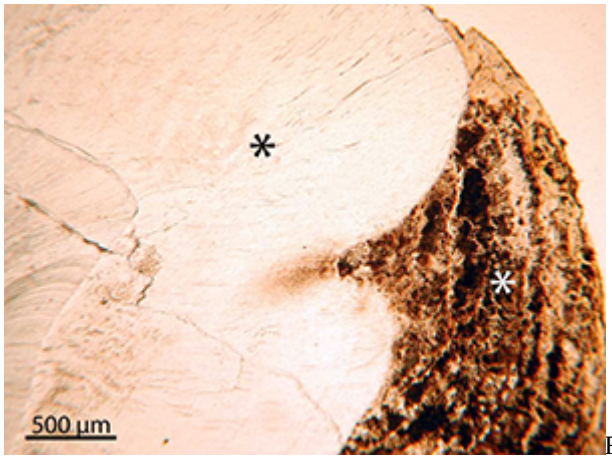

Figure 54: Micrograph of sample EIN-10. A thick layer of calculus (white asterisk) overlies the enamel (black asterisk)

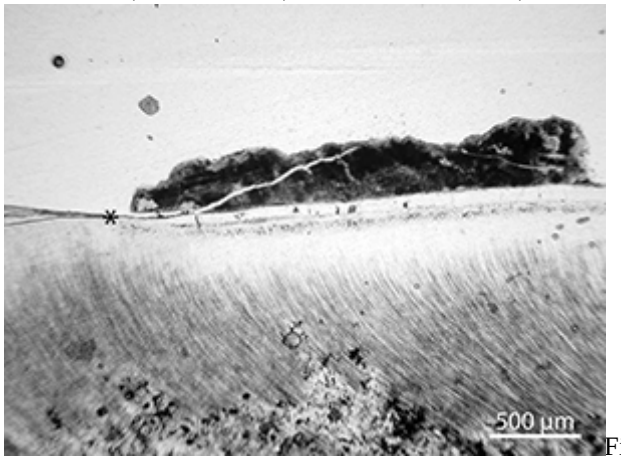

Figure 55: Micrograph of sample EIN-12. Calculus overlying the cementum just below the enamel-cementum junction (asterisk).

4.6 What is this? Unknown features observed

A variety of features unknown to us were observed in the tooth thin-sections. We would appreciate feedback from readers who may be able to identify what is seen in the following micrographs.

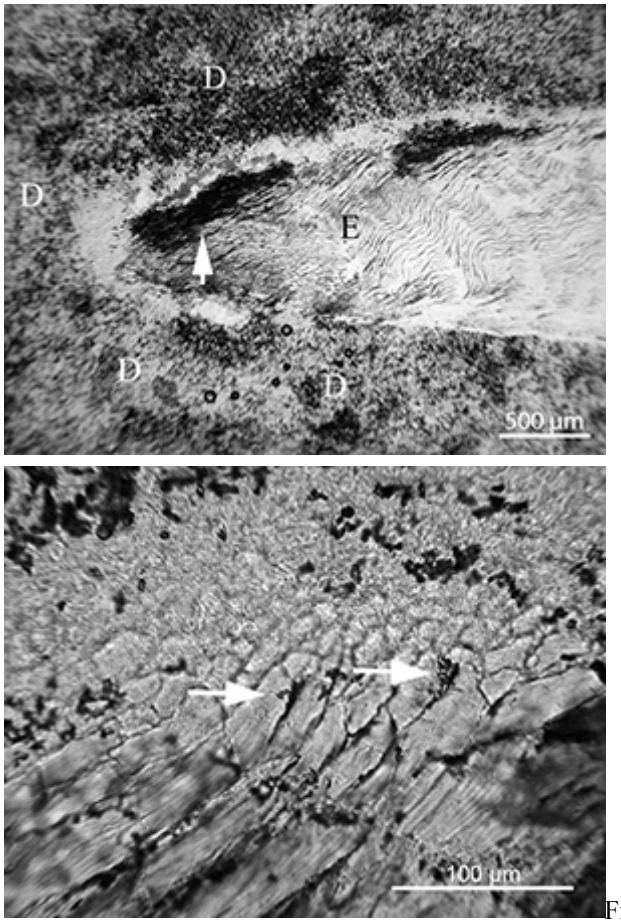

Figure 56: Tunnel-like features (white arrows) within the enamel of CDU-15 (cattle tooth). Could this be evidence of bioerosion in the enamel? The dentine is affected by intense bioerosion, going right up to the dentino-enamel junction whereas the enamel also exhibits extensive cracking. The tunnel-like features appear to emerge from the cracks. In Figure 56 the dark area does indicate cracks/tunnels filled with some opaque material. It is difficult to tell the features apart and further investigation would be needed to establish the nature of these. See also detail at higher magnification in Figure 57. (Image credit: H. Hollund)

Figure 57: Tunnel-like features (white arrows) within the enamel of CDU-15 (cattle tooth). Could this be evidence of bioerosion in the enamel? See also Figure 56. (Image credit: H. Hollund)

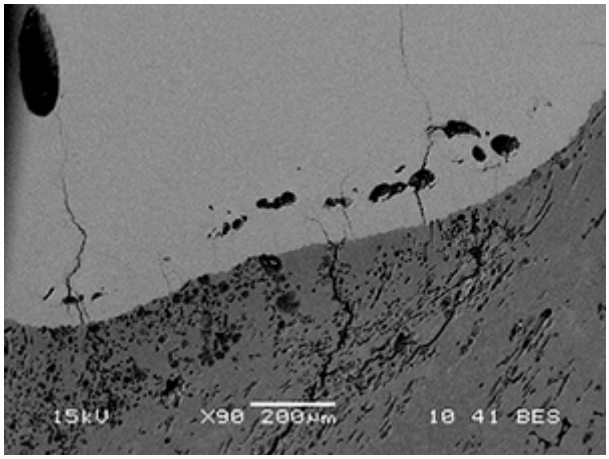

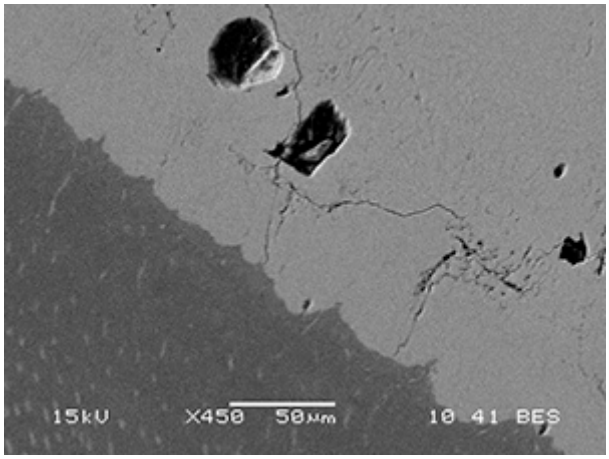

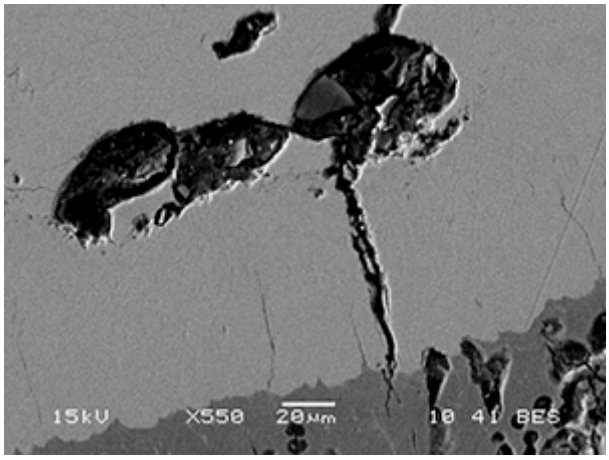

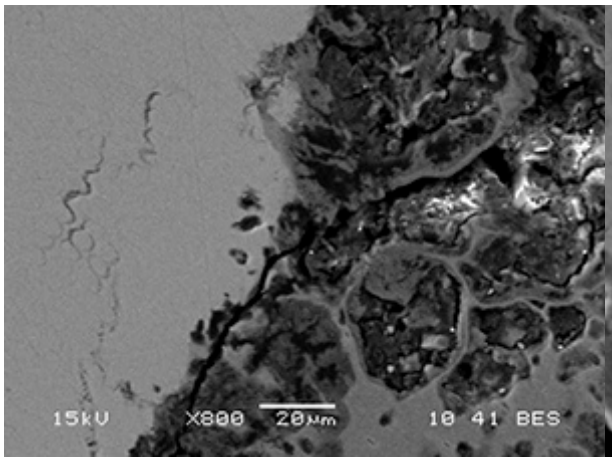

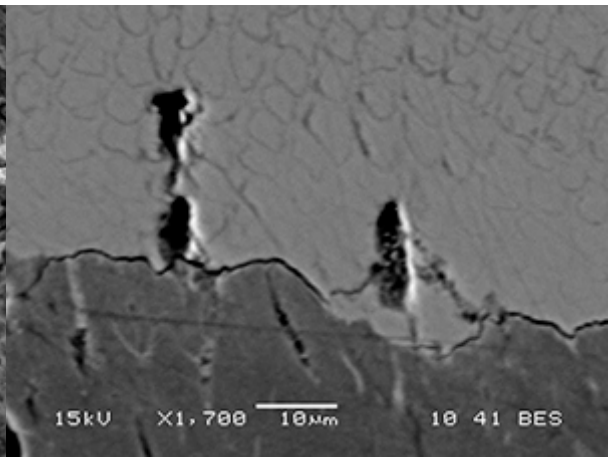

Figure 58: SEM-BSE images of globular cavities in the enamel of EIN-22. These are roughly 10-30 micron large, some empty, some containing inclusions. The cavities are located relatively close to the dentino-enamel junction and are sometimes associated with cracks. In several places the dentine is heavily bioeroded up to the dentino-enamel junction, where smaller cavities can be seen just on the border (Figure 61). See also Figures 59, 60 and 61. (Image credit: H. Hollund)

Figure 59: SEM-BSE images of globular cavities in the enamel of EIN-22. These are roughly 10-30 micron large, some empty, some containing inclusions. The cavities are located relatively close to the dentino-enamel junction and are sometimes associated with cracks. In several places the dentine is heavily bioeroded up to the dentino-enamel junction, where smaller cavities can be seen just on the border (Figure 61). See also Figures 58, 60 and 61. (Image credit: H. Hollund)

Figure 60: SEM-BSE images of globular cavities in the enamel of EIN-22. These are roughly 10-30 micron large, some empty, some containing inclusions. The cavities are located relatively close to the dentino-enamel junction and are sometimes associated with cracks. In several places the dentine is heavily bioeroded up to the dentino-enamel junction, where smaller cavities can be seen just on the border (Figure 61). See also Figures 58, 59 and 61. (Image credit: H. Hollund)

Figure 61: SEM-BSE images of globular cavities in the enamel of EIN-22. These are roughly 10-30 micron large, some empty, some containing inclusions. The cavities are located relatively close to the dentino-enamel junction and are sometimes associated with cracks. In several places the dentine is heavily bioeroded up to the dentino-enamel junction. Here, smaller cavities can be seen just on the border. See also Figures 58, 59 and 60. (Image credit: H. Hollund)

Figure 62: SEM-BSE images of globular cavities in the enamel of EIN-22. These are roughly 10-30 micron large, some empty, some containing inclusions, relatively close to the dentino-enamel junction and sometimes associated with cracks. (Image credit: H. Hollund)

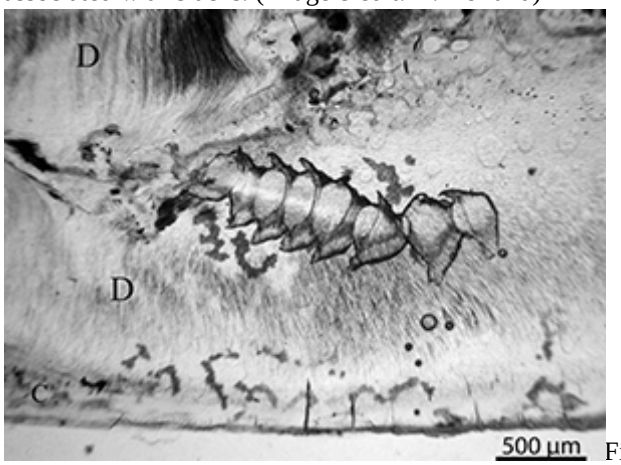

Figure 63: Micrograph showing the remains of an insect within human tooth CAS-08. The insect must have been located in the pulp cavity, but as a result of how the tooth was cut it appears here as superimposed on the dentine. Our knowledge does not allow us to identify species and we also do not know how it got there; during decomposition, or perhaps post-excavation, in storage. Identifying such remains may give important information on taphonomy, season of burial etc.

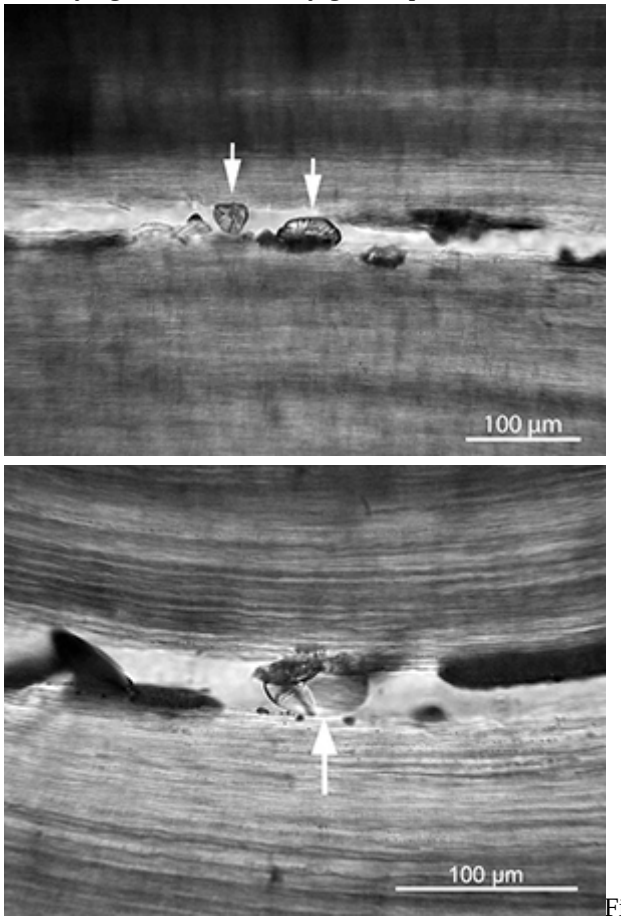

Figure 64: Micrograph showing unknown inclusions in a crack in CAS-08. Considering that this tooth also contained the remains of an insect (Figure 63), could these be insect eggs? See also Figure 65. (Image credit: H. Hollund)

Figure 65: Micrograph showing unknown inclusions in a crack in CAS-08. Considering that this tooth also contained the remains of an insect (Figure 63), could this be an insect egg? See also Figure 64. (Image credit: H. Hollund)

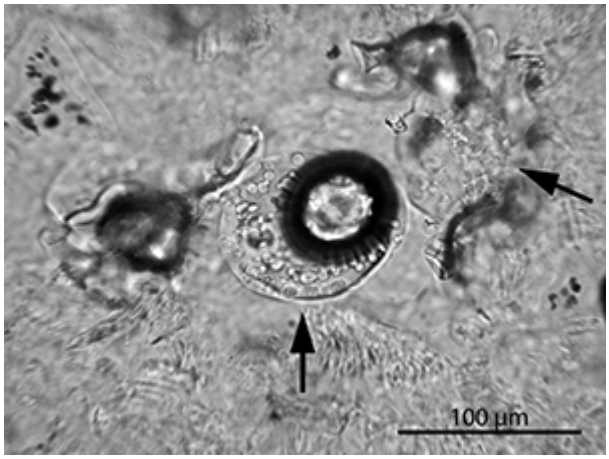

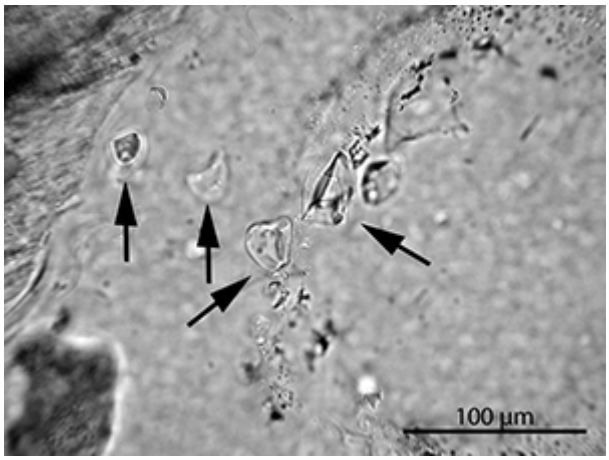

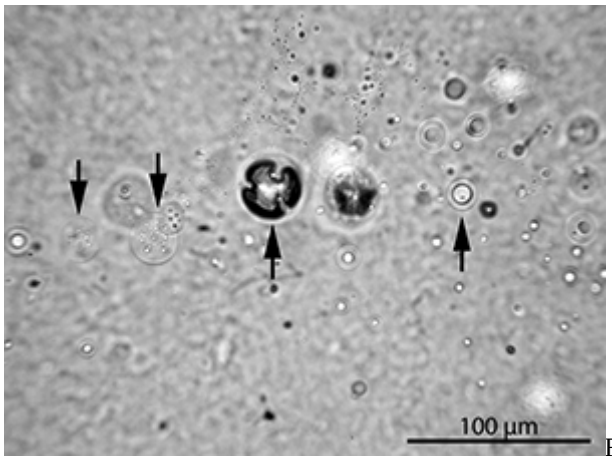

Figure 66: Micrograph of inclusions within the pulp cavity of EIN-23. These inclusions represent a variety of sizes and shapes. Most are probably fungal spores, spore sacks and yeast cells. The possibility that some of the circular features are air bubbles cannot be excluded. See also Figures 67 and 68. (Image credit: H. Hollund)

Figure 67: Micrograph of inclusions within the pulp cavity of EIN-23. These inclusions represent a variety of sizes and shapes. Most are probably fungal spores, spore sacks and yeast cells. The possibility that some of the circular features are air bubbles cannot be excluded. The dark circle in the middle of the image is an air bubble. See also Figures 66 and 68. (Image credit: H. Hollund)

Figure 68: Micrograph of inclusions within the pulp cavity of EIN-23. These inclusions represent a variety of sizes and shapes. Most are probably fungal spores, spore sacks and yeast cells. The possibility that some of the circular features are air bubbles cannot be excluded. The dark circle in the middle of the image is an air bubble. See also Figures 66 and 67. (Image credit: H. Hollund)

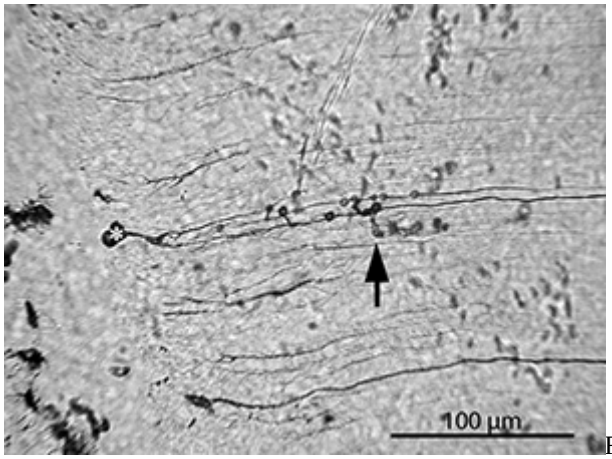

Figure 69: Micrograph of sample EIN-10 showing cuffed circular shapes located along the length of two dentinal tubuli. Some of the circles appear directly on the tubuli, others at the end of what looks like enlarged lateral branches. In addition a possible microbial tunnel, similar to what has been observed in many of the teeth, is emerging from one of the tubuli (arrow). The globular shape at the end of the tubuli where it meets the layer of Tomes and the cemento-dentinal junction, may also be an MFD (asterisk)

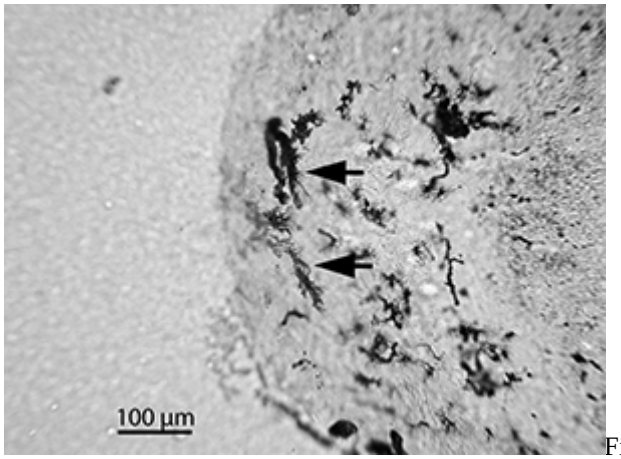

Figure 70: This micrograph of an area of cementum in EIN-23 shows cementocyte lacunae that seem bloated and enlarged, with tree-like structures and fine branches emerging from them. Could these be MFD caused by microbes?

5. Discussion

5.1 Bioerosion

The photo catalogue gives a visual impression as to how tooth diagenesis may compare to what is known of bone diagenesis. In contrast to what can be observed in bone (compare for example with Jans (2005) and Hedges *et al*. (1995), none of the analysed teeth has suffered complete destruction of the microstructure and all display histological indexes greater than 1. In other words, all of the teeth contained histologically pristine areas making up at least more than 15% of the total section surface studied. For bone, Hedges *et al*. (1995) observed a bimodal distribution in terms of histological integrity; the material preserves either very well or very poorly when considering microbial attack. If bioerosion happens in bone, it tends to go to 'completion'. Approximately 20% out of a large bone assemblage analysed (n = 139) displayed OHI of 0 or 1 (Hedges *et al*. 1995). The Eindhoven bone samples display the same pattern. For the teeth, we observe a similar bimodal distribution, but between 'medium' and 'excellent' in terms of the bioerosion index (Figure 71). If this is a representative pattern, it may be support for the idea that skeletal elements further from the abdomen preserve better (Jans *et al*. 2004; Child 1995) as teeth are further away than femora, on the premise that endogenous gut bacteria are involved in eroding the skeleton (see discussion further below). Consequently, teeth

contain larger areas of well-preserved tissue once environmental conditions have been established that inhibit further microbial activity. Alternatively/additionally, the difference in the microstructure, including the lower number of cell cavities, the lack of connection via canaliculi and the layer of Tomes at the cemento-dentinal junction, may slow down progress into the tissue. Finally, the enamel and the surrounding bone will protect the cementum/dentine from attack by soil microorganisms. Sognnaes (1950) found that the teeth he studied were increasingly affected by bioerosion with increase in post-mortem age, testifying to the role of aerobic soil-bacteria in post-mortem decay. Turner-Walker (2008) similarly considers aerobic soil bacteria the cause of most tunnelling seen in bone and teeth. However, it has also been suggested that extensive bone bioerosion may occur early post-mortem as part of putrefactive processes while soft tissues are still present (Yoshino *et al*. 1991; Bell *et al*. 1991; Jans 2005), making gut bacteria the potential 'perpetrators. Internal invasion by bacteria suggests the action of microbes travelling by the inter-connected vascular system. We also observed internal invasion in some of the teeth where bacteria mainly enter via the apex and the pulp cavity (Figures 8 and 9). It is not yet clear, however, if such a pattern can be assigned to endogenous bacteria. Soil bacteria may also be able to enter deep into the bone and teeth via the groundwater, while an inhibiting environment at the outer surfaces of the skeletal elements prevents them from utilising the areas close to the outer surfaces. Furthermore, the cementum does not contain pores connected to the surface as the pulp cavity surface does and the latter may thus be the route of least resistance. However, tunnelling from the cementum surface was also observed (Figure 9, Figure 10 and Figure 14). Another interesting observation is that the only clear fungal tunnelling observed (Wedl type tunnels) was in one of the cattle teeth. Although it is a single observation, it corroborates the findings of Jans *et al*. (2004) where fungal tunnelling was the dominant type in bones of slaughtered animals and was not observed as frequently in human bones. The authors suggested several explanations including differences in structure and porosity in human and animal bones, as well as differences in burial contexts and pre-excavation treatments such as slaughtering (thus removing the gut, the source of putrefactive bacteria).

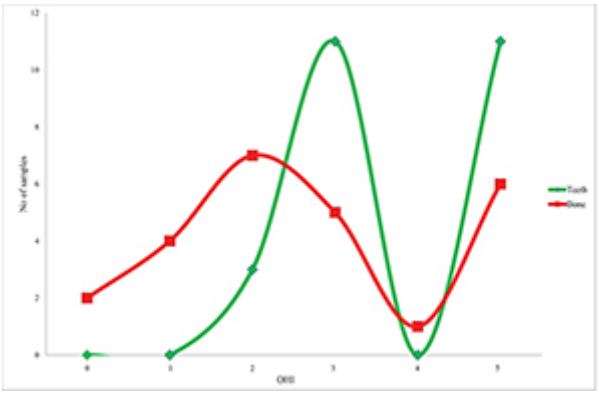

Figure 71: Graph showing the biomodal distribution of the Oxford histological index (OHI) values for bone and teeth from the site of Eindhoven.

Little is known of the species involved in bioerosion of skeletal material and the processes by which the organisms alter the material. It is furthermore not clear what the different morphological categories of MFD represent; different species, or different stages of tunnelling. In less severely attacked teeth, where individual tunnels can be more easily studied, a range of shapes are apparent that seem to relate to the type of tissue and the orientation of the mineralised collagen, but also stages of progression of bacteria into the tissue. For example, enlarged cementocyte canaliculi and tubuli and narrower canals, can be seen to expand into wider, more globular shapes. Another shape frequently observed consisted of connected, oblong shapes (Figure 11), again suggesting the progressive invasion of bacterial colonies. A further shape that may be linked to bacterial decay relates to the enlarged canaliculi, sometimes expanding into longer, 'bloated' branches of a cementocyte lacunae, as observed in Figure 13 and possibly in Figure 66. In Figure 18, Figure 19 and Figure 20, features can be seen that are similar to budded tunnels observed in bone. The focal destructions in the teeth show the same features with 1 micron-sized cavities in a demineralised zone surrounded by a hypermineralised border, as observed in bone MFD (Jackes *et al*. 2001). Hackett (1981) described budded tunnels in bone to be

around 30 micron in diameter, whereas these MFD are much larger, up to roughly 300 micron. The size may relate to the difference in microstructure in bone and dentine as the osteonal system may provide a restriction in MFD size in bone. Contrary to what Turner-Walker (2008) observed, both globular and elongated shapes are found in the dentine, as seen in Figure 11. There is in sum a large variety of morphologies of MFD observed, from branching tree- or bush-like shapes, enlarged canaliculi and tubuli, sometimes with a small bulb at the end and demineralised zones with borders and cavities, of various shapes and sizes.

An advantage of teeth in the investigation of post-mortem bacterial destruction is that examples of similar processes can be found in the literature on dental pathologies. An experimental study by Nyvad and Fejerskov (1990) demonstrated that actively progressing cementum caries lesions show a gradient of demineralisation and are invaded by bacteria. They observed that the bacterial activity mainly occurred between groups of relatively well-mineralised extrinsic collagen fibres. The cemento-dentinal junction furthermore seemed to form a barrier to bacterial penetration into the dentine which could be explained by the presence of a narrow hypermineralised zone and/or the abrupt change in collagen fibre orientation at the junction (Nyvad and Fejerskov 1990). The cemento-dentinal junction has recently been described as an enamel-like, hypermineralised zone containing little organics (Cherian 2011). Nyvad and Fejerskov (1990) found that in a few cases, bacteria would penetrate into the dentine, keeping to the dentinal tubuli and their lateral branches. *In-vivo*, this process is inhibited, as a bacterial presence in the tubuli will cause a cellular response that closes the tubuli to protect the dental pulp (Broncker pers. comm.). That fibre orientation plays a role also for post-mortem bacterial attack in teeth is clear from the patterns found in the present study. However, bacterial tunnels are also observed crossing the cemento-dentinal junction (Figure 10). Additionally, some features could be interpreted as microbial tunnelling extending into the enamel (Figures 54, 55, 56, 57 and 58), further discussed below. In addition to the microbial tunnels, the unknown insect and fungal-like inclusions observed (Figures 62, 63, 64, 65, 66, 67 and 68) serves as an illustration of the complex set of organisms probably colonising the material at several different stages throughout the post-mortem history of the material. When these processes are better understood, teeth and bone will constitute an even richer archive of taphonomic and environmental information.

5.2 Generalised destruction, infiltrations and inclusions

Chemically similar to bone, dentine and cementum are also sensitive to mineral dissolution, in extreme cases suffering complete destruction of the microstructure and subsequent cracking (large cracks) and loss of material as seen in Figures 45, 46 and 47. However, the tooth in Figure 45 provides a striking example of how well the enamel protects against non-biological decay, retaining a pristine area directly beneath the protective enamel crown despite severe destruction of the root. Furthermore, the cementum and dentine are, like bone, prone to infiltration of both organic (e.g. humic factors) and inorganic (e.g. iron oxides) material, often observed as staining. In several well-preserved teeth the staining occurred only in the cementum. Various minerals, organic inclusions and other types of material from the surrounding soil may fill cavities, pores and cracks in the tissues. The presence of manganese/iron stains and inclusions within the teeth studied is not surprising, as both elements are commonly found within bone pores (Williams and Potts 1988). The precipitation of manganese in nature is primarily controlled by microbial activity (Toner *et al*. 2005) and several of the inorganic inclusions observed are probably biominerals, as indicated by close association with fungal remains and empty bacterial MFD (Figures 23, 33, 42). This is interesting as size, morphology and structure of such minerals may be characteristic of different microbial species (Santelli *et al*. 2011). This may be an as yet unexplored source of taphonomic information in archaeological skeletons.

In Hollund *et al*. (2012a) we showed that teeth were markedly better preserved in terms of generalised destruction based on higher average values for the General Histological Index than the bone samples. Only a couple of teeth display what could be called micro-fissures, similar to those found in bone. However, these are most likely sample preparation effects. The reason for the lower occurrence of micro-fissuring in teeth compared to bone is unknown but may relate to differences in microstructure

and the often better preservation of the organic phase. Turner-Walker (2011) found that tensile strength of bone was dependent on collagen content, lower collagen content giving lower tensile strength, consequently making the material more prone to cracking. In addition one could imagine that the physical protection offered by the enamel and the location in the alveolus limit expansion and absorb some of the impacting forces.

5.3 Enamel

In contrast to dentine, the enamel was frequently fissured. Enamel is a hard but brittle material that may readily crack both during burial and sample preparation (cutting, polishing and volume changes upon drying of the embedding media). The enamel was furthermore frequently affected by superficial staining and etching.

In two teeth, human and cattle, morphological features observed within the enamel may be the result of post-mortem microbial activity (Figures 58, 59, 60, 61 and 62). Similar features have, to our knowledge, never been described before, indeed nor has any microbial boring within the enamel. On the contrary, several authors note that even in cases of severe bioerosion in dentine and cementum, the enamel is not attacked (Bell *et al*. 1991; Kierdorf *et al*. 2009; Kalthoff *et al*. 2011). This is also what we have observed in the majority of severely bioeroded teeth; the attack stops by the dentino-enamel border. Thus, further investigation is needed to confirm the nature of these features. Boring within the enamel close to the dentine is not unimaginable since the tufts, stretching out into the enamel from the dentino-enamel border contain greater concentration of proteins than the rest of the enamel (Nanci 2003). Underwood *et al*. (1999) note the occurrence of borings in the enamel of severely attacked fossil fish teeth, but limited to the area around the crown-root junction where the enamel is thin. Furthermore, bioerosion is frequently found in mollusc shells, consisting of between 90-95% calcium carbonate and less than 5% protein (Zhang and Zhang 2006), where the destruction has been observed both as caries-like pitting and branching tunnels (Hook and Golubic 1993; Raghukumar *et al*. 1989).

5.4 Pathologies and diagenesis

No clear relationship was observed between the occurrence of caries and calculus and post-mortem bioerosion. However, both attrition and severe carious lesions in the enamel will expose the dentine to different agents of decay. Observations within one tooth suggest that bacteria may take advantage of less mineralised inter-globular dentine (Figure 22). We know that bacteria will exploit planes of weakness and less mineralised areas; thus it is to be expected that some pathologies leave teeth more vulnerable to diagenesis.

Caries lesions can be confidently identified if there is a reaction in the dentine directly underneath (Poole and Tratman 1978), as seen in Figures 45, 49 and 50, whereas superficial surface lesions, as illustrated in Figures 26 and 50, may not be easily distinguishable from diagenetic etching.

5.5 How are teeth better?

In sum, teeth seem to have greater potential than bone for containing areas of well-preserved tissue, despite extensive attack. This may explain why the analytical success rate concerning ancient DNA has been reported to be higher in teeth (see review in Hollund *et al*. 2012a), as diagenetic 'niches' within teeth may contain well-preserved DNA (Geigl 2002; Hiller *et al*. 2004; Hollund 2013; Salamon et al. 2005). However, as can be seen in Figure 9, bioerosion may cause severe destruction of large areas, including the crown dentine, owing to invasions via the pulp cavity. Although none of the teeth in this assemblage showed the most severe level of decay, very few remained unaffected. Only four out of the 34 samples (12%) displayed the best GHI score of 5 (considering both bioerosion and generalised destruction). Furthermore, teeth may be dislocated from the alveolar socket, affected by attrition or severe carious lesions, directly exposing the cementum and dentine to the environment.

Adler *et al*. (2011) recommends the cementum as source material tissue for ancient DNA analyses owing to higher initial DNA concentrations compared to dentine. This would only hold true for exceptionally well-preserved teeth, as the cementum is frequently affected both by biological and non-biological processes of decay. Alternatively, if the invasion is internal, as seen in Figure 8, the cementum/surface areas would be the better material to sample. As such, a recommendation of which part of the tooth to be sampled for archaeometric analyses can only be carried out after diagenetic analyses have established overall preservation and the main agent(s) of decay involved. In our previous paper (Hollund *et al*. 2012a), we suggested that this can be carried out on the corresponding bone if teeth are not available for diagenetic screening. However, due to intra-skeletal variation in state of preservation and to minimise destruction of unique remains, the ideal would be a sampling strategy adjusted to allow the destruction of only one tooth for several types of analyses, including histology and ancient DNA assays.

6. Conclusions

This study has presented an inventory of post-mortem alterations in archaeological teeth observable at histological scale. Various types of diagenetic alterations are observed. Our previous study showed that the variation in diagenesis may result from tissue types, differences in taphonomic processes and specific burial conditions. Here, a photo catalogue has been made that can aid other workers within the fields of archaeology, palaeontology and forensics. In general, the study illustrates how dental tissue suffers from the same diagenetic issues as bone and sometimes to a severe degree. In addition, dental elements may be made more vulnerable to post-mortem diagenesis as a result of pathologies. Consequently, dental tissues should also be screened before any further chemical and molecular analysis. As suggested for bone, the pattern of microbial attack may indicate the pathway of bacterial/fungal attack, also suggesting timing, before or after skeletonisation of the remains. However, a fairly limited set of samples was used and larger, more systematic characterisation of the type of histological alterations occurring in teeth is needed. To improve understanding of the observed features, chemical and mineralogical analysis of infiltrations and inclusions would be of great value, as well as high-resolution 3-D imaging of microbial tunnelling and microbial DNA analysis.

The differences and similarities found between bone and dental diagenesis can be summarised as follows:

- Similar tunnel morphologies and type of inclusions (organic and inorganic) are observed.
- As with bone, microbes may attack from external or internal surfaces.
- Severe bioerosion can be found in teeth but this seems to leave comparatively larger areas unaffected than in bone.
- No completely bioeroded tooth was observed whereas complete bioerosion is relatively common in bone.
- As in bone, tunnelling microbes/bacteria respect the microarchitecture of dentine and cementum. However, tunnels were observed that crossed the more crystalline layer of Tomes. Additionally, possible enamel tunnelling was observed.
- Generalised destruction, staining and inclusions (both organic and inorganic) may affect bone and teeth to a similar degree.
- Several not previously described morphological features, presumably relating to microbial activity have been observed in the current assemblage of teeth, including possible enamel tunnelling. Further investigations are necessary to confirm their nature.
- Dentine and cementum are rarely affected by microfissuring whereas this is a common occurrence in bone and enamel.

Acknowledgements

The sample material was contributed by the Archaeology Section of the city of Eindhoven (NL), the Archaeology Section of Noord-Holland, National Corporation for Antiquities and Museums, Khartoum (Sudan) and Le Historial de la Vendee (France). The following persons are acknowledged for facilitating sampling: Nico Arts (Eindhoven Archaeology section), Rob van Eerden (Noord-Holland Archaeology section), Vincent Francigny, Alex de Voogt (American Museum of Natural History, New York), Eveline Altena (Leiden University), Lisette Kootker (VU University Amsterdam), Marie Soressi (Centre Archéologique d'Orléans), Roger Joussaume, Sophie Corson (Le Historial de la Vendee) and Frederick Feulner (University of York). The authors also wish to thank Wynanda Koot (VU University, Amsterdam) for sample preparation and Ineke Joosten (National Cultural Heritage Agency, Amsterdam) for carrying out the SEM analyses.

The research was conducted within the framework of a Marie Curie Training Network, LECHE (7th Framework Programme, project number 215362) and mostly carried out during a PhD studentship at the Institute of Geo- and Bioarchaeology, the VU University, Amsterdam (NL).

Bibliography

Adler, C.J., Haak, W., Donlon, D. and Cooper, A. 2011 'Survival and recovery of DNA from ancient teeth and bones', *Journal of Archaeological Science* **38**, 956-64. http://dx.doi.org/10.1016/j.jas.2010.11.010

Alaeddini R., Walsh S. J., Abbas A. 2010 'Forensic implications of genetic analyses from degraded DNA-A review', *Forensic Science International: Genetics* **4**, 148-157. http://dx.doi.org/10.1016/j.fsigen.2009.09.007

Bell, L. S., Boyde, A., Jones, S. J. 1991 'Diagenetic alteration to teeth in situ illustrated by backscattered electron imaging', *Scanning* **13**, 173-83. http://dx.doi.org/10.1002/sca.4950130204

Bocherens, H., Polet, C. and Toussaint, M. 2007 'Palaeodiet of Mesolithic and Neolithic populations of Meuse Basin (Belgium): evidence from stable isotopes', *Journal of Archaeological Science* **34**, 10-27. http://dx.doi.org/10.1016/j.jas.2006.03.009

Breen A. P., Murphy J. A. 1995 'Reactions of oxyl radicals with DNA', *Free Radical Biology and Medicine* **18**: 1033-1077. http://dx.doi.org/10.1016/0891-5849(94)00209-3

Britton, K., Grimes, V., Dau, J. and Richards, M.P. 2009 'Reconstructing faunal migrations using intra-tooth sampling and strontium and oxygen isotope analyses: a case study of modern caribou', *Journal of Archaeological Science* **36**, 1163-72. http://dx.doi.org/10.1016/j.jas.2009.01.003

Burford, E.P., Hillier, S. and Gadd, G.M. 2006 'Biomineralization of fungal hyphae with calcite (CaCO3) and calcium oxalate mono- and dihydrate in carboniferous limestone microcosms', *Geomicrobiology Journal* **23**, 599-611. http://dx.doi.org/10.1080/01490450600964375

Cherian, G. 2011 'Harvesting cementum from root surface: a new paradigm in the study of cementum and the cemento-dentinal junction', *Journal of Advanced Dental Research* **2**, 17-20. Available: http://www.joaor.org/userfiles/Vol-2-Issue-2-May-Aug-2011/03George.pdf

Child, A.M. 1995 'Towards an understanding of the microbial decomposition of archaeological bone in the burial environment', *Journal of Archaeological Science* **22**, 165-74. http://dx.doi.org/10.1006/jasc.1995.0018

Fernández-Jalvo, Y., Andrews, P., Pesquero, D., Smith, C., Marín-Monfort, D., Sánchez, B., Geigl, E.-M. and Alonso, A. 2010 'Early bone diagenesis in temperate environments: Part I: surface features and histology', *Palaeogeography, Palaeoclimatology, Palaeoecology* **288**, 62-81. http://dx.doi.org/10.1016/j.palaeo.2009.12.016

Feulner, F., Kootker, L.M., Hollund, H.I., Davies, G.R. and Craig, O.E. 2012 'Combined isotope analysis indicate restricted mobility of cattle at the Neolithic causewayed enclosure of Champ-Durand, Vendee (France)' in R. Joussaume (ed) *L'Enciente neolithique de Champ-Durand a Nieul-sur-l'Autise*. 549-61.

Garland, A.N. 1987 'A histological study of archaeological bone decomposition' in A. Boddington, A.N. Garland and R.C. Janaway (eds) *Death, Decay and Reconstruction. Approaches to Archaeology and Forensic Science*, Manchester: Manchester University Press. 109-26.

Garland, A.N. 1993 'An introduction to the histology of exhumed mineralized tissue' in G. Grupe and A.N. Garland (eds) *Histology of Ancient Human Bone: Methods and Diagnosis*, New York: Springer-Verlag. 1-16. http://dx.doi.org/10.1007/978-3-642-77001-2_1

Geigl, E.M. 2002 'On the circumstances surrounding the preservation and analysis of very old DNA', *Archaeometry* **44**, 337-42. http://dx.doi.org/10.1111/1475-4754.t01-1-00066

Gilbert, T.P.M., Rudbeck, L., Willerslev, E., Hansen, A.J., Smith, C., Penkman, K.E.H., Prangenberg, K., Nielsen-Marsh, C.M., Jans, M.E., Arthur, P., Lynnerup, N., Turner-Walker, G., Biddle, M., Kjølbye-Biddle, B. and Collins, M.J. 2005 'Biochemical and physical correlates of DNA contamination in archaeological human bones and teeth excavated at Matera, Italy', *Journal of Archaeological Science* **32**, 785-93. http://dx.doi.org/10.1016/j.jas.2004.12.008

Grupe, G. and Dreser-Werringloer, U. 1993 'Decomposition phenomena in thin-sections of excavated human bones' in G. Grupe and A.N. Garland (eds) *Histology of Ancient Human Bone: Methods and Diagnosis. Proceedings of the Paleohistology Workshop held from 3-5 October 1990 at Gottingen*, Berlin Heidelberg: Springer-Verlag. 27-36.

Hackett, C.J. 1981 'Microscopical focal destruction (tunnels in exhumed human bones)', *Medical Science Law* **21**, 243-65. http://dx.doi.org/10.1177/002580248102100403

Hedges, R.E.M., Millard, A.R. and Pike, A.W.G. 1995 'Measurements and relationships of diagenetic alteration of bone from three archaeological sites', *Journal of Archaeological Science* **22**, 201-9. http://dx.doi.org/10.1006/jasc.1995.0022

Hedges, R. E. M. 2002 'Bone diagenesis: an overview of processes', *Archaeometry* **44**, 319-328. http://dx.doi.org/10.1111/1475-4754.00064

Hiller, J.C., Collins, M.J., Chamberlain, A.T. and Wess, T.J. 2004 'Small-angle X-ray scattering: a high-throughput technique for investigating archaeological bone preservation', *Journal of Archaeological Science* **31**, 1349-59. http://dx.doi.org/10.1016/j.jas.2004.02.013

Hillson, S. 1986 *Teeth*, Cambridge: Cambridge University Press.

Hinz, E.A. and Kohn, M.J. 2010 'The effect of tissue structure and soil chemistry on trace element uptake in fossils', *Geochimica et Cosmochimica Acta* **74**, 3213-31. http://dx.doi.org/10.1016/j.gca.2010.03.011

Hollund, H.I. 2013 *Diagenetic Screening of Bone Samples; tools to aid taphonomic and archaeometric investigations*, Amsterdam, Department for Geo- and Bioarchaeology. Available: http://dare.ubvu.vu.nl/handle/1871/40245

Hollund, H.I., Arts, N., Jans, M.M.E. and Kars, H. 2012a 'Are Teeth Better? Histological Characterization of Diagenesis in Archaeological Bone–Tooth Pairs and a Discussion of the Consequences for Archaeometric Sample Selection and Analyses', *International Journal of Osteoarchaeology*. http://dx.doi.org/10.1002/oa.2376

Hollund, H.I., Jans, M.M.E., Collins, M.J., Kars, H., Joosten, I. and Kars, S.M. 2012b 'What happened here? Bone histology as a tool in decoding the postmortem histories of archaeological bone from Castricum, The Netherlands', *International Journal of Osteoarchaeology* **22**, 537-48. http://dx.doi.org/10.1002/oa.1273

Hook, J.E. and Golubic, S. 1993 'Microbial shell destruction in deep-sea mussels, Florida escarpment', *Marine Ecology* **14**, 81-89. http://dx.doi.org/10.1111/j.1439-0485.1993.tb00366.x

Jackes, M., Sherburne, R., Lubell, D., Barker, C. and Wayman, M. 2001 'Destruction of microstructure in archaeological bone: a case study from Portugal', *International Journal of Osteoarchaeology* **11**, 415-32. http://dx.doi.org/10.1002/oa.583

Jans, M.M.E. 2005 *Histologial Characterisation of Diagenetic Alteration of Archaeological Bone*, Amsterdam, Department for Geo- and Bioarchaeology.

Jans, M.M.E., Nielsen-Marsh, C.M., Smith, C.I., Collins, M.J. and Kars, H. 2004 'Characterisation of microbial attack on archaeological bone', *Journal of Archaeological Science* **31**, 87-95. http://dx.doi.org/10.1016/j.jas.2003.07.007

Kalthoff, D.C., Rose, K.D. and Von Koenigswald, W. 2011 'Dental microstructure in Palaeanodon and Tubulodon (Palaeanodonta) and bioerosional tunneling as a widespread phenomenon in fossil mammal teeth', *Journal of Vertebrate Paleontology* **31**, 1303-13. http://dx.doi.org/10.1080/02724634.2011.607997

Kierdorf, H., Kierdorf, U., Witzel, C., Intoh, M. and Dobney, K., 2009 'Developmental defects and postmortem changes in archaeological pig teeth from Fais Island, Micronesia', *Journal of Archaeological Science* **36**, 1637-46. http://dx.doi.org/10.1016/j.jas.2009.03.028

King C. E., Debruyne R., Kuch M., Schwarz C., Poinar H. N. 2009 'A quantitative approach to detect and overcome PCR inhibition in ancient DNA extracts', *BioTechniques* **47**, 941-949. http://dx.doi.org/10.2144/000113244

Marchiafava, V., Bonucci, E. and Ascenzi, A. 1974 'Fungal osteoclasia: a model of dead bone resorption', *Calcified Tissue International* **14**, 195-210. http://dx.doi.org/10.1007/bf02060295

Marsland, E.A. and Browne, R.M. 1975 *Colour Atlas of Oral Histopathology*, Aylesbury: H.M. + M. Publishers.

Meyer, E., Wiese, M., Bruchhaus, H., Claussen, M. and Klein, A. 2000 'Extraction and amplification of authentic DNA from ancient human remains', *Forensic Science International* **113**, 87-90. http://dx.doi.org/10.1016/s0379-0738(00)00220-6

Nanci, A. 2003 *Ten Cates Oral Histology: Development, Structure, and Function*, St Louis: Mosby corp.

Nyvad, B. and Fejerskov, O. 1990 'An ultastructural study of bacterial invasion and tissue breakdown in human experimental root-surface caries', *Journal of Dental Research* **69**, 1118-25. http://dx.doi.org/10.1177/00220345900690050101

Piperno, D.R., Weiss, E., Holst, I. and Nadel, D. 2004 'Processing of wild cereal grains in the Upper Palaeolithic revealed by starch grain analysis', *Nature* **430**, 670-73. http://dx.doi.org/10.1038/nature02734

Pitre, M.C., Mayne Correia, P., Mankowski, P.J., Klassen, J., Day, M.J., Lovell, N.C. and Currah, R. 2013 'Biofilm growth in human skeletal material from ancient Mesopotamia', *Journal of Archaeological Science* **40**, 24-29. http://dx.doi.org/10.1016/j.jas.2012.06.022

Poole, D.F.G. and Tratman, E.K. 1978 'Post-mortem changes in human teeth from late upper Palaeolithic/Mesolithic occupants of an English limestone cave', *Archives of Oral Biology* **23**, 1115-20. http://dx.doi.org/10.1016/0003-9969(78)90117-6

Raghukumar, C., Rao, V.P.C. and Iyer, S.D. 1989 'Precipitation of iron in windowpane oyster shells by marine shell-boring Cyanobacteria', *Geomicrobiology Journal* **7**, 235-44. http://dx.doi.org/10.1016/0003-9969(78)90117-610.1080/01490458909377869

Rosvold, J., Halley, D.J., Hufthammer, A.K., Andersen, R. and Minagawa, M. 2010 'The rise and fall of wild boar in a northern environment: evidence from stable isotopes and subfossil finds', *Holocene* **20**, 1113-21. http://dx.doi.org/10.1177/0959683610369505

Salamon, M., Tuross, N., Arensburg, B., Weiner, S. and Arsuaga, J.L. 2005 'Relatively well preserved DNA is present in the crystal aggregates of fossil bones', *Proceedings of the National Academy of Sciences of the United States of America* **102**, 13783-88. http://dx.doi.org/10.1073/pnas.0503718102

Santelli, C.M., Webb, S.M., Dohnalkova, A.C. and Hansel, C.M. 2011 'Diversity of Mn oxides produced by Mn(II)-oxidizing fungi', *Geochimica et Cosmochimica Acta* **75**, 2762-76. http://dx.doi.org/10.1016/j.gca.2011.02.022

Sognnaes, R.F. 1950 'Postmortem microscopic defects in the teeth of ancient man', *Archives of Pathology* **59**, 559-70.

Sponheimer, M. and Lee-Thorp, J.A. 2006 'Enamel diagenesis at South African Australopith sites: implications for paleoecological reconstruction with trace elements', *Geochimica et Cosmochimica Acta* **70**, 1644-54. http://dx.doi.org/10.1016/j.gca.2005.12.022

Toner, B., Fakra, S., Villalobos, M., Warwick, T. and Sposito, G. 2005 'Spatially resolved characterization of biogenic manganese oxide production within a bacterial biofilm', *Applied Environmental Microbiology* **71**, 1300-10. http://dx.doi.org/10.1128/AEM.71.3.1300-1310.2005

Trueman, C.N. and Martill, D.M. 2002 'The long-term survival of bone: the role of bioerosion', *Archaeometry* **44**, 371-82. http://dx.doi.org/10.1111/1475-4754.t01-1-00070

Turner-Walker, G. 2008 'The chemical and microbial degradation of bones and teeth' in R. Pinhasi and S. Mays (eds) *Advances in Human Paleopathology*, Chichester: John Wiley and Sons Ltd. 3-29.

Turner-Walker, G. 2011 'The mechanical properties of artificially aged bone: probing the nature of the collagen-mineral bond', *Palaeogeography, Palaeoclimatology, Palaeoecology* **310**, 17-22. http://dx.doi.org/10.1016/j.palaeo.2011.03.024

Turner-Walker, G. 2012 'Early bioerosion in skeletal tissues: persistence through deep time', *Neues Jahrbuch fur Geologie und Palaontologie - Abhandlungen* **265**, 165-83. http://dx.doi.org/10.1127/0077-7749/2012/0253

Underwood, C.J., Mitchell, S.F. and Veltkamp, C.J. 1999 'Microborings in mid Cretaceous fish teeth', *Proceedings of the Yorkshire Geological Society* **52**, 269-74. http://dx.doi.org/10.1144/pygs.52.3.269

Van Klinken G. J., Hedges R. E. M. 1995 'Experiments on collagen-humic interactions: Speed of humic uptake, and effects of diverse chemical treatments', *Journal of Archaeological Science* **22**, 263-270. http://dx.doi.org/10.1006/jasc.1995.0028

Williams, C.T. and Potts, P.J. 1988 'Research notes and application reports. Element distribution maps in fossil bones', *Archaeometry* **30**, 237-47. http://dx.doi.org/10.1111/j.1475-4754.1988.tb00450.x

Yoshino, M., Kimijima, T., Miyasaka, S., Sato, H. and Seta, S. 1991 'Microscopical study on estimation of time since death in skeletal remains', *Forensic Science International* **49**, 143-58. http://dx.doi.org/10.1016/0379-0738(91)90074-S

Zhang, C. and Zhang, R. 2006 'Matrix proteins in the outer shells of molluscs', *Marine Biotechnology* **8**, 572-86. http://dx.doi.org/10.1007/s10126-005-6029-6